Studying $D^0 \to 4\pi^\pm$ with CLEO-c data

Contents

1 Event selection

$D^0 \to 4\pi^\pm$ candidates are selected with both fully- and partially-reconstructed tags.

1.1 Selection of $D^0 \to 4\pi^\pm$

Standard $D^0 \to 4\pi^\pm$ candidates are selected with the `DTag` software. The ΔE of this tag must lie within ± 0.025 GeV (this is the cut used by CLEO-c in PRL 96 (2006) 081802 (`hep-ex/0512063`)). No further cuts are applied to the final-state pions. A D^0-constrained mass fit is performed and the resulting pion 4-momenta are used to determine Dalitz plot variables. The χ^2 of this fit must be greater than zero.

1.2 Selection of fully-reconstructed opposite-side tags

This section describes the selections used for each opposite-side tag. The same cuts are used for both single and double tags.

Cuts on ΔE are shown in Table 1.

Decay mode	Min. ΔE (GeV)	Max. ΔE (GeV)
K^+K^-	-0.0200	0.0200
$\pi^+\pi^-$	-0.0300	0.0300
$K^\pm\pi^\mp$	-0.0294	0.0294
$K^0_S\pi^0$	-0.0710	0.0450
$K^0_S\eta$	-0.0550	0.0350
$K^0_S\omega$	-0.0250	0.0250
$K^0_S\eta'$	-0.0300	0.0200
$K^0_S\pi^0\pi^0$	-0.0550	0.0450
$K^\pm\pi^\mp\pi^0$	-0.0583	0.0350
$\pi^+\pi^-\pi^0$	-0.0583	0.0350
$K^0_S\pi^+\pi^-$	-0.0200	0.0200

Table 1: ΔE cuts.

Any tag containing a K^0_S has the following cuts applied:

- K^0_S flight significance > 2.0,
- $0.4901 < m(K^0_S) < 0.5051$ GeV/c^2,
- For $K^0_S\omega$ only, $\cos(\theta_{K^0_S}) > 0.7$.

Any tag containing a π^0 or η candidate decaying to $\gamma\gamma$ has the following cut applied:

- E9/E25 OK for both high and lower energy showers.

Mass cuts are applied to the following final-state particles:

- $0.506 < m(\eta) < 0.590$ GeV/c^2,
- $0.762 < m(\omega) < 0.802$ GeV/c^2,
- $0.950 < m(\eta') < 0.964$ GeV/c^2.

Lepton and shower vetos are **not** applied to the h^+h^- final states.

A D^0 mass fit is applied to the $K^0_S\pi^+\pi^-$ final state. The χ^2 of this fit must be ≥ 0.

1.3 Multiple candidate selection

When there are multiple double-tagged candidates in an event, the candidate with the smallest value of a particular metric is selected. If the double-tag is continuum-dominated (K^+K^-, $\pi^+\pi^-$, $\pi^+\pi^-\pi^0$, $4\pi^\pm$) the metric is

$$\left|\Delta E(D_1^0) + \Delta E(D_2^0)\right|.$$

In all other modes the metric is

$$\left|\frac{m_{\rm BC}(D_1^0) + m_{\rm BC}(D_2^0)}{2} - m_{D^0}^{\rm PDG}\right|.$$

The use of ΔE for the continuum-dominated modes is necessary because a fit is performed to the average $m_{\rm BC}$ of the double tags. Selecting based on average $m_{\rm BC}$ will bias events towards the signal region, artificially increasing the signal yield. Both types of selection have been tried and the only tag affected significantly is $4\pi^\pm$.

1.4 K_S^0 veto

It is important to veto $K_S^0\pi^+\pi^-$ backgrounds to $4\pi^\pm$. All K_S^0 candidates in each event are selected. Their descendant pions are compared to those of the D^0 candidate, using the internal numerical identifier. If both pions have matching identifiers with any pair of D^0 descendants, the K_S^0 must have a negative flight significance or the event is rejected.

This is an effective cut but it is important to consider genuine $4\pi^\pm$ candidates that match a fake $K_S^0\pi^+\pi^-$ candidate and are rejected unnecessarily. As long as the FS cut doesn't prefer certain regions of phase space this is fine. A mass cut on the K_S^0 might cause a bias.

The K_S^0 veto is applied after the multiple candidate selection. The K_S^0 veto is more likely to remove 'signal-like' candidates that lie in the signal region; when there are multiple candidates, this often leaves candidates that lie in the diagonal sideband. Applying the multiple candidate selection beforehand negates this problem, and the K_S^0 veto is still useful.

A veto is applied to the $\pi^+\pi^-\pi^0$ final state in order to reject $K_S^0\pi^0$ backgrounds. The same method and selection criteria are used.

When selecting $4\pi^\pm$ against $4\pi^\pm$, three K_S^0 vetos are considered:

- K_S^0 FS < 0,
- K_S^0 FS < -2,
- K_S^0 mass further than 7.5 MeV/c^2 from the PDG value.

1.5 Selection of single tags

Single tags are selected using the `DTag` framework. The cuts listed in Section 1.2 are applied, in addition to lepton and shower vetos for the h^+h^- final states. The K^+K^- final state also has the following cut applied:

- `NOT`$\{-0.93 < \cos\theta(K^-) < -0.90$ `AND` $0.90 < \cos\theta(K^+) < 0.93\}$.

1.6 Selection of partially-reconstructed final states

The $4\pi^\pm$ candidate reconstructed against a partially-reconstructed final state has these cuts applied to it:

- $|\Delta E| < 0.025$ GeV/c^2,
- $1.86 < m_{\rm BC} < 1.87$ GeV/c^2,
- K_S^0 veto, requiring flight significance < 0.

Decay mode	Low sideband (GeV/c^2)		Signal region (GeV/c^2)		High sideband (GeV/c^2)	
	Min.	Max.	Min.	Max.	Min.	Max.
$K^0_L\pi^0$	-0.1	0.05	0.1	0.5	0.6	1.0
$K^0_L\omega$	0.0	0.1	0.15	0.35	0.4	1.2
$K^0_L\pi^+\pi^-$	0.0	0.15	0.2	0.3	0.45	0.8

Table 2: $m^2_{\rm miss}$ cuts.

When there are multiple candidates in an event, the one with the smallest value of $|m_{\rm BC} - m^{\rm PDG}_{D^0}|$ is selected. As with the fully-reconstructed states, the K^0_S veto is applied after the multiple candidate selection.

Cuts on $m^2_{\rm miss}$ are listed in Table 2. These are a bit different to the ones used in the $K^0_S K^+ K^-$ analysis, mainly to ensure the sidebands are fully representative of the spread in background types.

A two-dimensional cut is placed on the plane of ($\cos\theta$, $E_{\rm shower}$) in order to reduce background from stray showers. The quantity $\cos\theta$ is the angle between an additional shower in the event and the inferred K^0_L momentum, and $E_{\rm shower}$ is the energy of the shower in question. An event is accepted if all additional showers satisfy one of the following criteria:

- $-1.0 \leq \cos\theta < 0.90$ and $E_{\rm shower} < 0.1$ GeV,
- $0.90 \leq \cos\theta < 0.98$ and $E_{\rm shower} < (2.5\cos\theta - 2.15)$ GeV.

The following mode-dependent cuts are additionally applied:

- $K^0_L\pi^0$
  - π^0 momentum between 0.75–1.0 GeV/c,
  - π^0 E9/E25 OK,
  - Only one π^0 found, no η found, no tracks found (excluding $4\pi^\pm$ `DTag`).
- $K^0_L\omega$
  - π^0 momentum between 0.15–0.6 GeV/c and E9/E25 OK,
  - $0.762 < m(\omega) < 0.802$ GeV/c^2,
  - Only one π^0 found, no η found, two tracks found (excluding $4\pi^\pm$ `DTag`).
- $K^0_L\pi^+\pi^-$
  - No π^0 found, no η found, two tracks found (in addition to $4\pi^\pm$ `DTag`).
  - A D^0 mass fit is applied to the $K^0_L\pi^+\pi^-$ final state. The χ^2 of this fit must be ≥ 0.

2 Fully-reconstructed selection results

2.1 Data yields

The number of candidates selected in data for each fully-reconstructed decay mode at different selection stages is shown in Table 3. The table also shows $B_{\rm flat}$, the quantity of flat background estimated from the sidebands. It is particularly significant for K^+K^-, $\pi^+\pi^-$, $\pi^+\pi^-\pi^0$ and $4\pi^\pm$. In these cases the dominant source of background is continuum production, for which an alternative strategy is used to determine the signal yields. The numbers are included here for completeness.

Decay mode	DTag		Cuts		K^0_S veto	On $m_{\rm BC}$ plane					$B_{\rm flat}$
	Cands.	Events	Cands.	Events	and MCS	S	A	B	C	D	
K^+K^-	751	751	175	175	106	34	4	0	36	0	23.7 ± 3.7
$\pi^+\pi^-$	2833	2813	581	579	490	83	0	0	204	10	120.1 ± 9.0
$K^\pm\pi^\mp$	1776	1764	1357	1355	659	600	0	3	6	1	4.4 ± 1.7
$K^0_S\pi^0$	533	509	236	231	132	120	1	0	1	0	1.0 ± 0.6
$K^0_S\eta(\gamma\gamma)$	246	234	50	48	25	20	1	0	0	0	0.4 ± 0.4
$K^0_S\omega$	19129	8631	101	101	51	44	0	0	1	0	0.6 ± 0.6
$K^0_S\eta(\pi^+\pi^-\pi^0)$	19129	8631	18	17	9	7	0	0	0	0	0.0
$K^0_S\eta'(\pi^+\pi^-\eta)$	53	40	19	18	12	10	0	1	0	0	0.4 ± 0.4
$K^0_S\pi^0\pi^0$	3290	2632	97	87	49	23	1	0	5	2	2.4 ± 1.6
$K^\pm\pi^\mp\pi^0$	6226	4691	3556	3116	1488	1223	20	7	34	12	25.4 ± 4.6
$\pi^+\pi^-\pi^0$	5670	4691	1111	1004	738	188	10	8	208	37	115.5 ± 9.6
$K^0_S\pi^+\pi^-$	12370	6978	637	550	297	248	0	1	20	2	11.6 ± 2.9
$4\pi^\pm$ (K^0_S FS < 0)	16737	9729	3176	2679	1937	344	2	1	814	44	478.2 ± 18.0
$4\pi^\pm$ (K^0_S FS < -2)	16737	9729	3176	2679	1493	257	2	1	623	34	366.1 ± 15.6
$4\pi^\pm$ (K^0_S mass veto)	16737	9729	3176	2679	2197	386	3	1	917	44	541.9 ± 19.1

Table 3: Candidate and event yields in data at various stages: '`DTag`' is number from `DTag` software, 'Cuts' is number after selection cuts, 'K^0_S veto and MCS' is number after K^0_S veto and multiple candidate selection have been applied. 'On $m_{\rm BC}$ plane' indicates number of candidates in each region on the $m_{\rm BC}$ plane. $B_{\rm flat}$ is the flat background estimate from the sidebands. For $4\pi^\pm$ against itself the K^0_S veto is applied to both sides.

2.2 Generic MC yields

The number of candidates selected in generic MC for each fully-reconstructed decay mode at different selection stages is shown in Table 4. In most cases the peaking $K^0_S\pi^+\pi^-$ vs tag background yield is between 7–10% of the signal yield. It is a bit larger for $4\pi^\pm$ vs $4\pi^\pm$ and $4\pi^\pm$ vs $\pi^+\pi^-\pi^0$ which is unsurprising.

2.3 Continuum MC yields

The number of candidates selected in continuum MC for each fully-reconstructed decay mode at different selection stages is shown in Table 5. The selection was not performed on most of the K^0_SX modes, which are not anticipated to have a large continuum contribution. This is borne out by the fact that hardly any events are selected as $K^0_S\pi^0$, which is the most populous of the K^0_SX modes.

As expected, the modes K^+K^-, $\pi^+\pi^-$, $\pi^+\pi^-\pi^0$ and $4\pi^\pm$ all have a large continuum contribution. The ratios of the yields in the C box to the S box are 3.1 ± 0.7, 2.4 ± 0.2, 2.5 ± 0.1 and 2.6 ± 0.4 respectively, which are all consistent.

Decay mode	DTag		Cuts		K^0_S veto	On $m_{\rm BC}$ plane						
	Cands.	Events	Cands.	Events	and MCS	S			A	B	C	D
						Sig	Peak	Other				
K^+K^-	4503	4498	2255	2253	1164	797	57	33	25	6	119	5
$\pi^+\pi^-$	1099	1089	877	876	439	380	27	2	4	2	0	0
$K^\pm\pi^\mp$	23618	23397	21196	21154	9954	8778	745	20	4	24	5	1
$K^0_S\pi^0$	4474	4317	2918	2883	1350	1119	102	11	2	3	7	0
$K^0_S\eta(\gamma\gamma)$	1089	993	486	471	227	149	13	10	14	1	2	2
$K^0_S\omega$	75998	31367	1284	1206	573	421	39	35	4	2	16	2
$K^0_S\eta(\pi^+\pi^-\pi^0)$	75998	31367	324	275	163	59	62	12	5	2	10	0
$K^0_S\eta'(\pi^+\pi^-\eta)$	414	336	220	210	88	72	5	0	0	0	0	1
$K^0_S\pi^0\pi^0$	7881	5615	1827	1563	737	374	32	66	18	3	51	18
$K^\pm\pi^\mp\pi^0$	88770	64185	55859	48689	23279	18155	1656	285	275	69	475	58
$\pi^+\pi^-\pi^0$	10511	7604	6242	5592	2750	1814	465	64	27	6	60	9
$K^0_S\pi^+\pi^-$	25270	13210	8670	7632	3763	3179	326	21	4	15	45	2
$4\pi^\pm$ (K^0_S FS < 0)	9369	4757	4509	3581	962	559	133	12	2	1	115	2
$4\pi^\pm$ (K^0_S FS < -2)	9369	4757	4509	3581	688	428	50	7	1	1	93	2
$4\pi^\pm$ (K^0_S mass veto)	9369	4757	4509	3581	1074	657	103	14	2	1	134	4

Table 4: Candidate and event yields in generic MC at various stages: '`DTag`' is number from `DTag` software, 'Cuts' is number after selection cuts, 'K^0_S veto and MCS' is number after K^0_S veto and multiple candidate selection have been applied. 'On $m_{\rm BC}$ plane' indicates number of candidates in each region on the $m_{\rm BC}$ plane. 'Sig' is the number of truth-matched $4\pi^\pm$ vs tag candidates, 'Peak' is the number of $K^0_S\pi^+\pi^-$ vs tag candidates, and 'Other' encompasses all remaining background candidates.

Decay mode	DTag		Cuts		K^0_S veto	On $m_{\rm BC}$ plane				
	Cands.	Events	Cands.	Events	and MCS	S	A	B	C	D
K^+K^-	1169	1168	189	189	171	24	0	0	75	1
$\pi^+\pi^-$	4567	4528	968	968	866	144	1	2	350	13
$K^\pm\pi^\mp$	950	946	133	133	40	4	1	1	21	1
$K^0_S\pi^0$	796	760	23	23	7	2	0	0	2	1
$K^\pm\pi^\mp\pi^0$	3039	2546	539	493	192	19	4	2	53	17
$\pi^+\pi^-\pi^0$	33076	26759	6633	6101	5213	776	16	33	1914	265
$K^0_S\pi^+\pi^-$	3466	2164	178	156	83	14	0	2	34	2
$4\pi^\pm$ (K^0_S FS < 0)	3503	2212	565	501	343	51	0	0	136	6
$4\pi^\pm$ (K^0_S FS < -2)	3503	2212	565	501	273	41	0	0	106	5
$4\pi^\pm$ (K^0_S mass veto)	3503	2212	565	501	410	64	0	0	161	8

Table 5: Candidate and event yields in continuum MC at various stages: '`DTag`' is number from `DTag` software, 'Cuts' is number after selection cuts, 'K^0_S veto and MCS' is number after K^0_S veto and multiple candidate selection have been applied. 'On $m_{\rm BC}$ plane' indicates number of candidates in each region on the $m_{\rm BC}$ plane.

The continuum MC is produced at 5× the luminosity of datasets 31–37, i.e. $5 \times 0.2815 = 1.408$ fb^{-1}. The scaling factor between this sample and the total collected in data is thus $0.8181/1.408 = 0.581$.

2.4 Signal MC

Various signal MC samples are generated with approximately 50k events per sample. Signal efficiencies are listed in Table 6. The events are required to lie in the $m_{\rm BC}$ vs $m_{\rm BC}$ signal region ($1.86 \leq m_{\rm BC} \leq 1.87$). Efficiencies are determined with respect to the number at generator level.

In addition the peaking background in which $K^0_S\pi^+\pi^-$ is reconstructed as $4\pi^\pm$ is important. The efficiencies of these modes are also tabulated and are consistently a few percent of the signal mode in question.

Decay mode	Reconstructed as	Efficiency (%)
$4\pi^\pm$ vs K^+K^-	Itself	27.2 ± 0.2
$4\pi^\pm$ vs $\pi^+\pi^-$	Itself	34.0 ± 0.2
$4\pi^\pm$ vs $K^\pm\pi^\mp$	Itself	31.0 ± 0.2
$4\pi^\pm$ vs $K^0_S\pi^0$	Itself	14.0 ± 0.2
$4\pi^\pm$ vs $K^0_S\eta(\gamma\gamma)$	Itself	12.9 ± 0.2
$4\pi^\pm$ vs $K^0_S\omega$	Itself	6.1 ± 0.1
$4\pi^\pm$ vs $K^0_S\eta(\pi^+\pi^-\pi^0)$	Itself	8.5 ± 0.1
$4\pi^\pm$ vs $K^0_S\eta'(\pi^+\pi^-\eta)$	Itself	6.8 ± 0.1
$4\pi^\pm$ vs $K^0_S\pi^0\pi^0$	Itself	6.5 ± 0.1
$4\pi^\pm$ vs $\pi^+\pi^-\pi^0$	Itself	20.1 ± 0.2
$4\pi^\pm$ vs $4\pi^\pm$ (K^0_S FS < 0)	Itself	20.3 ± 0.2
$4\pi^\pm$ vs $4\pi^\pm$ (K^0_S FS < -2)	Itself	15.2 ± 0.2
$4\pi^\pm$ vs $4\pi^\pm$ (K^0_S mass veto)	Itself	23.7 ± 0.2
$4\pi^\pm$ vs $K^0_S\pi^+\pi^-$	Itself	15.7 ± 0.2
$K^0_S\pi^+\pi^-$ vs K^+K^-	$4\pi^\pm$ vs K^+K^-	0.4 ± 0.0
$K^0_S\pi^+\pi^-$ vs $\pi^+\pi^-$	$4\pi^\pm$ vs $\pi^+\pi^-$	0.6 ± 0.0
$K^0_S\pi^+\pi^-$ vs $\pi^+\pi^-\pi^0$	$4\pi^\pm$ vs $\pi^+\pi^-\pi^0$	0.5 ± 0.0
$K^0_S\pi^+\pi^-$ vs $4\pi^\pm$	$4\pi^\pm$ vs $4\pi^\pm$	0.7 ± 0.0
$4\pi^\pm$ vs $K^0_S\pi^0$	$4\pi^\pm$ vs $\pi^+\pi^-\pi^0$	0.4 ± 0.0

Table 6: Signal MC efficiencies for fully-reconstructed decay modes.

The efficiencies for $4\pi^\pm$ vs $4\pi^\pm$ with different K^0_S vetos are in the same proportion as the number of signal events found in the generic MC (Table 4).

2.5 Thrust

The cosine of the angle between the thrust vectors of the two `DTag` candidates, $\cos(\theta_{\rm thr})$, can potentially be used to discriminate between continuum events and genuine signal. Continuum events will be approximately collinear and thus the cosine will be close to 1.

Figures 1 and 2 show the distribution of each double-tag on the $m_{\rm BC}$ plane in data. Peaks around 1 are clearly observed.

Figures 3 and 4 show the distribution of each double-tag on the $m_{\rm BC}$ plane in MC. Both generic and continuum MC are shown on the same plot. The continuum MC has been scaled by 8.4 which is the relative size of the two MC-data scaling factors.

In general the continuum MC has the same behaviour: approximately linear from $-1.0 < \cos(\theta_{\rm thr}) < 0.6$ and steeply rising thereafter. The truth-matched signal has a gentle upward slope across the entire $\cos(\theta_{\rm thr})$ range.

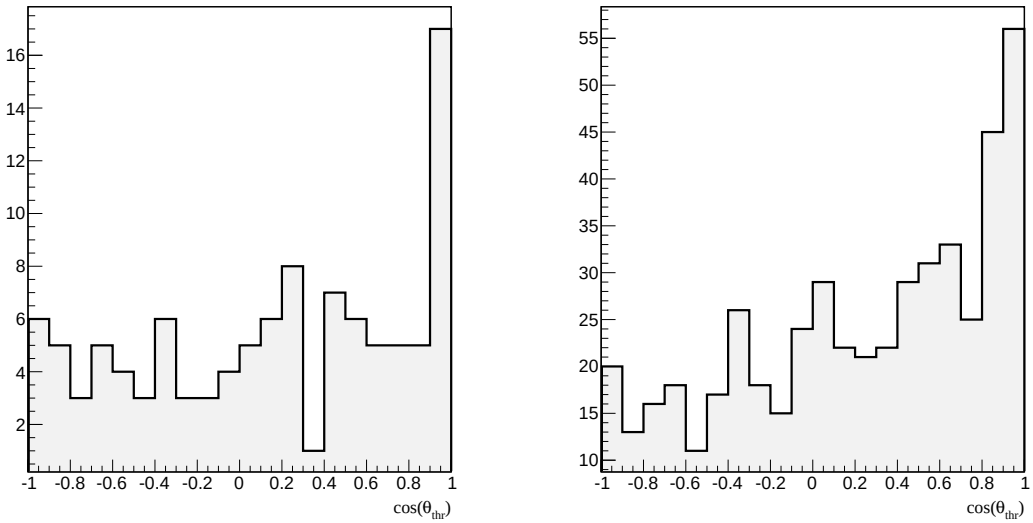

Figure 1: $\cos(\theta_{\rm thr})$, for $4\pi^{\pm}$ tagged with (left) K^+K^- (right) $\pi^+\pi^-$ in data.

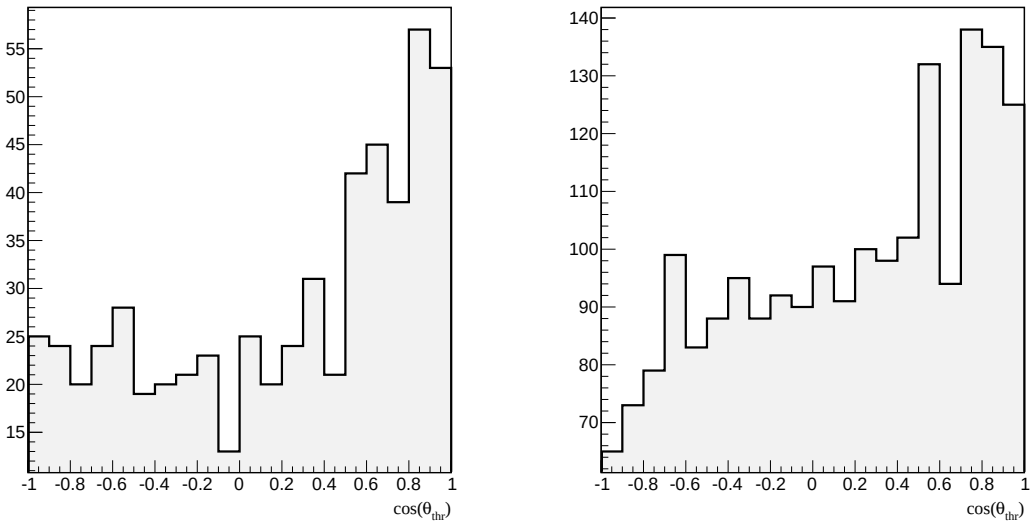

Figure 2: $\cos(\theta_{\rm thr})$, for $4\pi^{\pm}$ tagged with (left) $\pi^+\pi^-\pi^0$ (right) $4\pi^{\pm}$ in data.

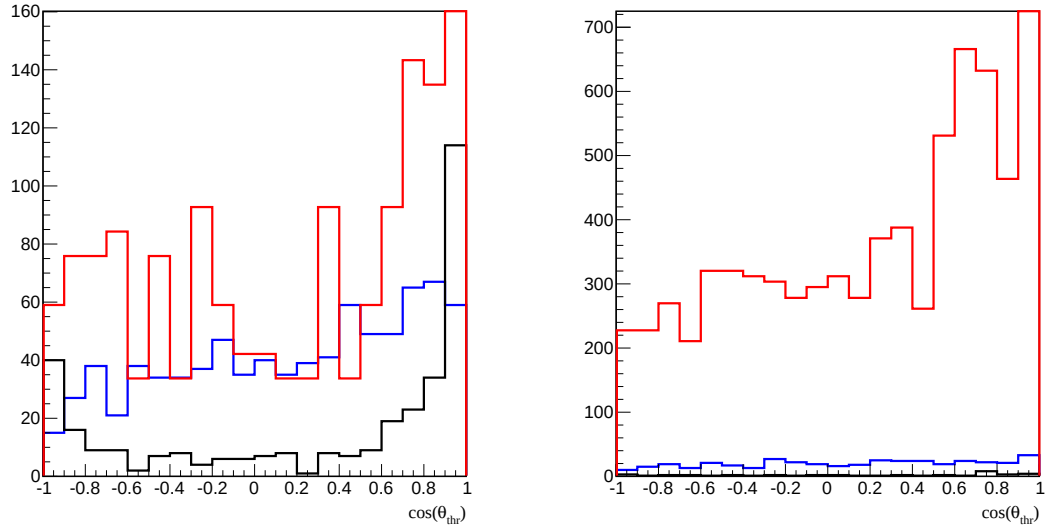

Figure 3: $\cos(\theta_{\rm thr})$, for $4\pi^{\pm}$ tagged with (left) K^+K^- (right) $\pi^+\pi^-$ in MC. The red line is scaled continuum MC, the blue line is truth-matched $4\pi^{\pm}$ vs tag in generic MC, and the black line is all backgrounds in generic MC.

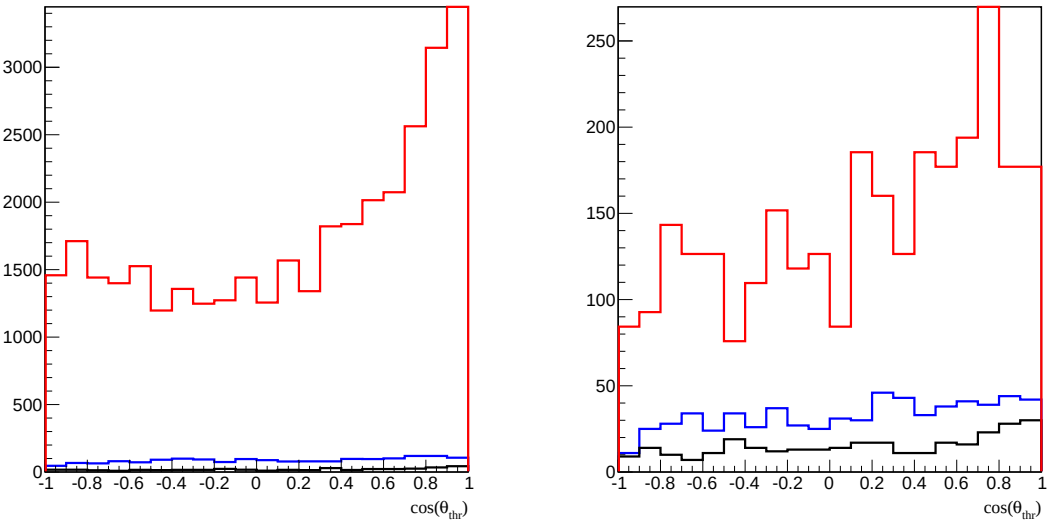

Figure 4: $\cos(\theta_{\rm thr})$, for $4\pi^{\pm}$ tagged with (left) $\pi^+\pi^-\pi^0$ (right) $4\pi^{\pm}$ in MC. The red line is scaled continuum MC, the blue line is truth-matched $4\pi^{\pm}$ vs tag in generic MC, and the black line is all backgrounds in generic MC.

The K^+K^- MC background behaves differently to that of the other three tags; there is a strong peak at 1 (and a smaller peak at -1) which matches the behaviour observed in data. A large number of these backgrounds are track-swapped $D^+(K^-\pi^+\pi^+)$ vs $D^-(K^+\pi^-\pi^-)$ events. D^+ vs D^- events have historically been taken to be part of the 'flat' background across the $m_{\rm BC}$ plane. This is a reasonable assumption to make; see Figure 12 in Section 2.7.

The effect of a cut on $\cos(\theta_{\rm thr})$, is evaluated by considering the metric $S/\sqrt{S+B}$ for a range of cuts. S is taken to be the quantity of truth-matched signal and B is taken to be the quantity of continuum background. The signal is scaled to data by a factor 0.0689 (which is the luminosity-weighted scaling factor for datasets 31–37 and 43–46) and the continuum background is scaled by a factor of 0.581. The generic MC background is ignored.

For each decay mode the best value of the metric is obtained without applying any cut. In reality the value of S will be lower for K^+K^- and $\pi^+\pi^-$ tags in particular because only the $CP-$ portion of $4\pi^\pm$ will be able to decay, but whether this will affect the conclusions is unclear. The use of thrust as a discriminating variable is not considered any further.

2.6 Data $m_{\rm BC}$ planes

Figures 5–11 show the distribution of each double-tag on the $m_{\rm BC}$ plane in data.

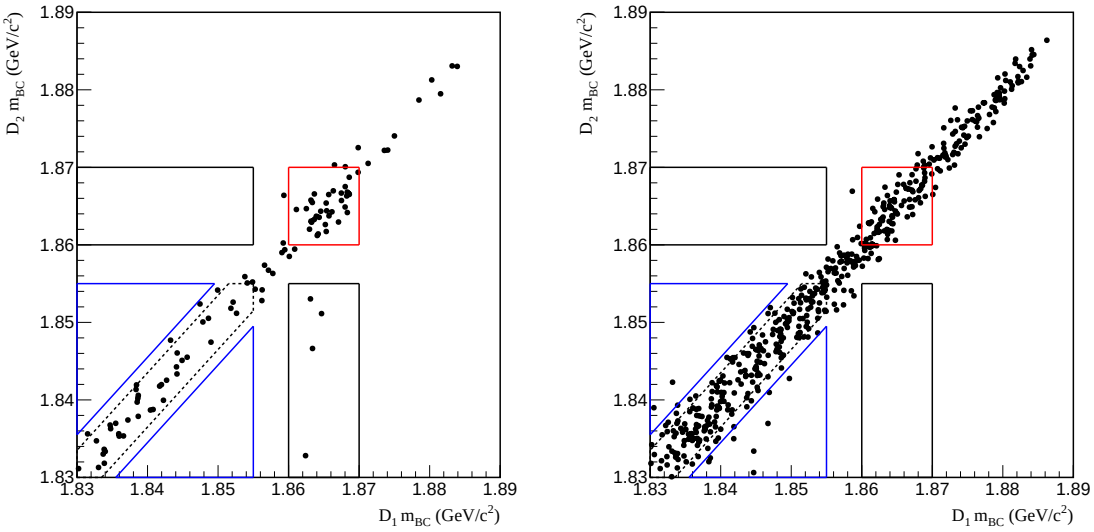

Figure 5: $m_{\rm BC}$ plane for $4\pi^\pm$ tagged with (left) K^+K^- (right) $\pi^+\pi^-$.

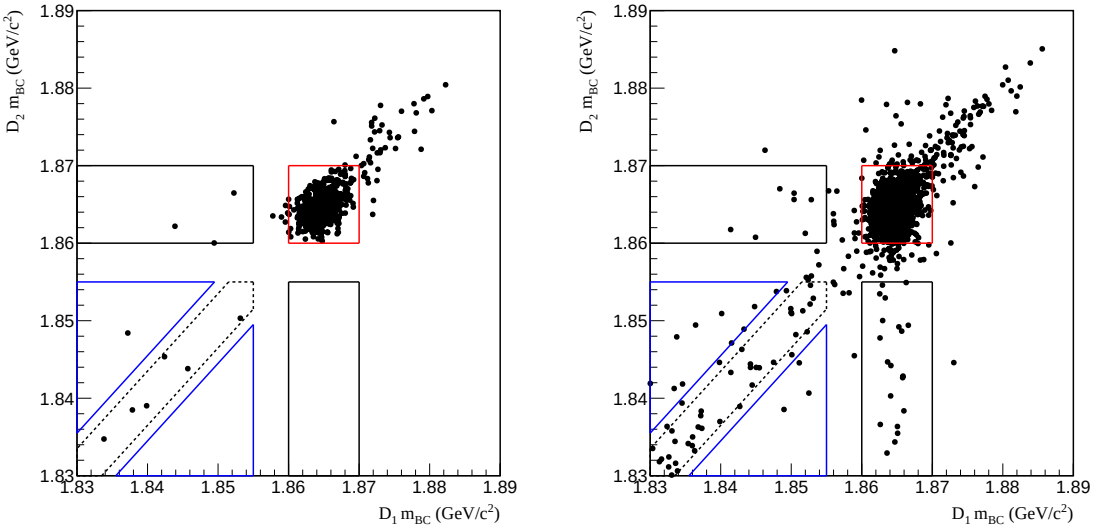

Figure 6: $m_{\rm BC}$ plane for $4\pi^{\pm}$ tagged with (left) $K^{\pm}\pi^{\mp}$ (right) $K^{\pm}\pi^{\mp}\pi^{0}$.

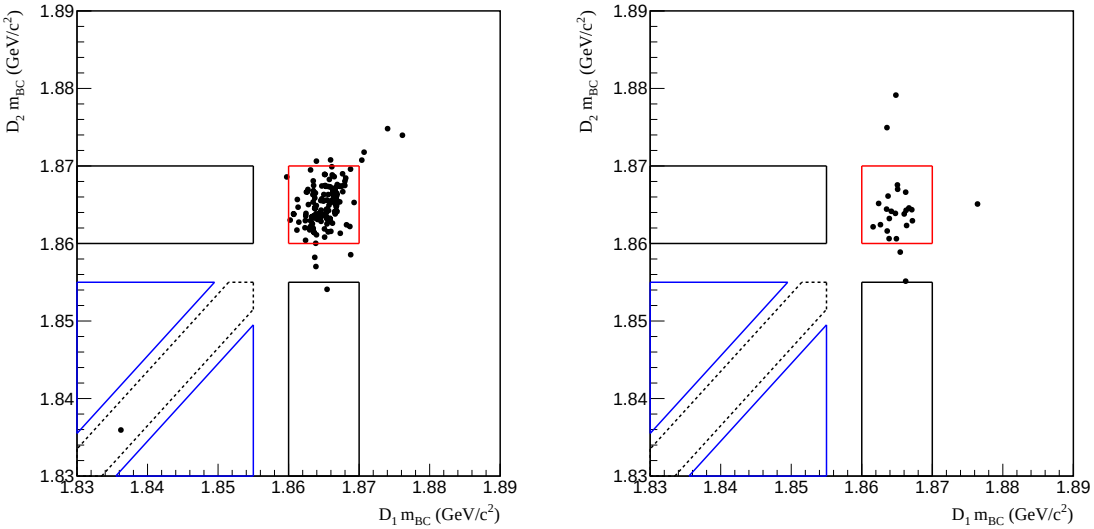

Figure 7: $m_{\rm BC}$ plane for $4\pi^{\pm}$ tagged with (left) $K^{0}_{S}\pi^{0}$ (right) $K^{0}_{S}\eta(\gamma\gamma)$.

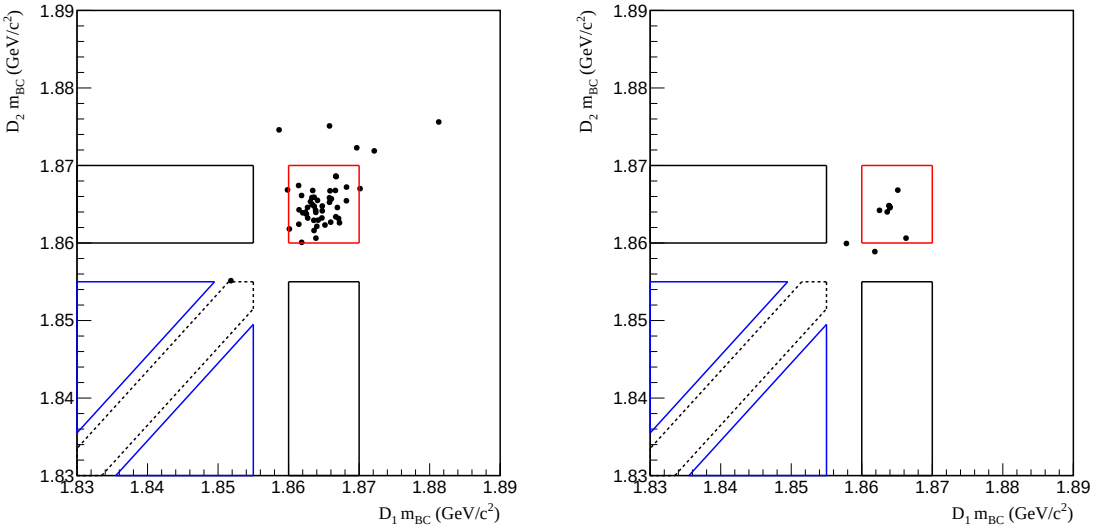

Figure 8: $m_{\rm BC}$ plane for $4\pi^{\pm}$ tagged with (left) $K^0_S\omega$ (right) $K^0_S\eta(\pi^+\pi^-\pi^0)$.

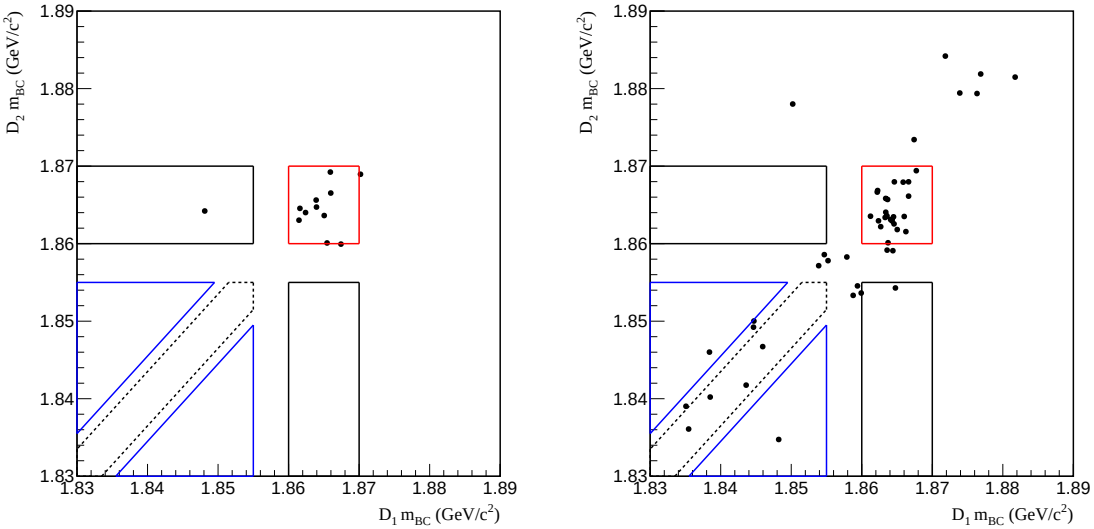

Figure 9: $m_{\rm BC}$ plane for $4\pi^{\pm}$ tagged with (left) $K^0_S\eta'(\pi^+\pi^-\eta)$ (right) $K^0_S\pi^0\pi^0$.

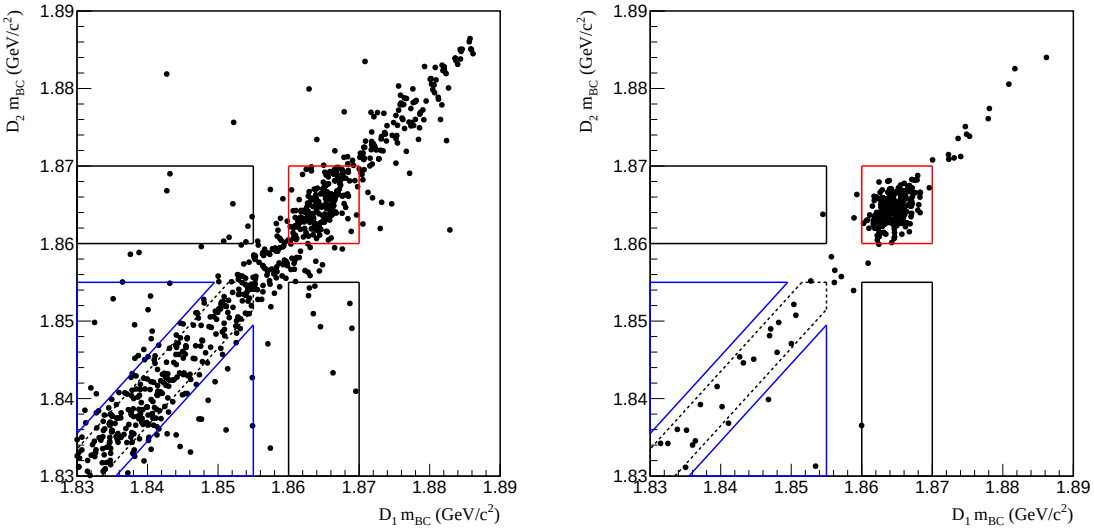

Figure 10: $m_{\rm BC}$ plane for $4\pi^{\pm}$ tagged with (left) $\pi^+\pi^-\pi^0$ (right) $K^0_S\pi^+\pi^-$.

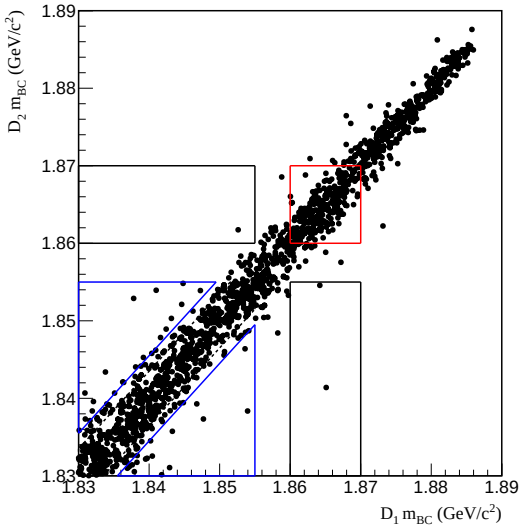

Figure 11: $m_{\rm BC}$ plane for $4\pi^{\pm}$ tagged with $4\pi^{\pm}$.

2.7 Generic MC $m_{\rm BC}$ planes

Figures 12–24 show the distribution of each double-tag on the $m_{\rm BC}$ plane in generic MC. The candidates are divided into signal, peaking background and other backgrounds. The D^+ vs D^- track-swapped background is shown separately for K^+K^-.

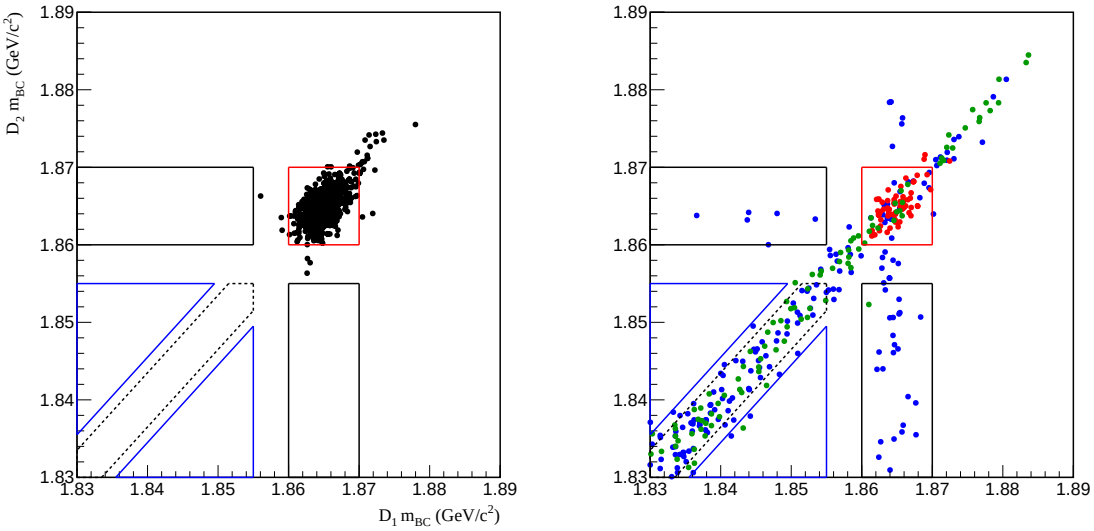

Figure 12: $m_{\rm BC}$ plane in generic MC for $4\pi^{\pm}$ tagged with K^+K^-. The left plot shows signal candidates, the right plot shows background candidates. The red points are the peaking $K^0_S\pi^+\pi^-$ vs K^+K^- background, the green points are D^+ vs D^- track-swapped background (particularly significant for K^+K^-) and the blue points are all other backgrounds.

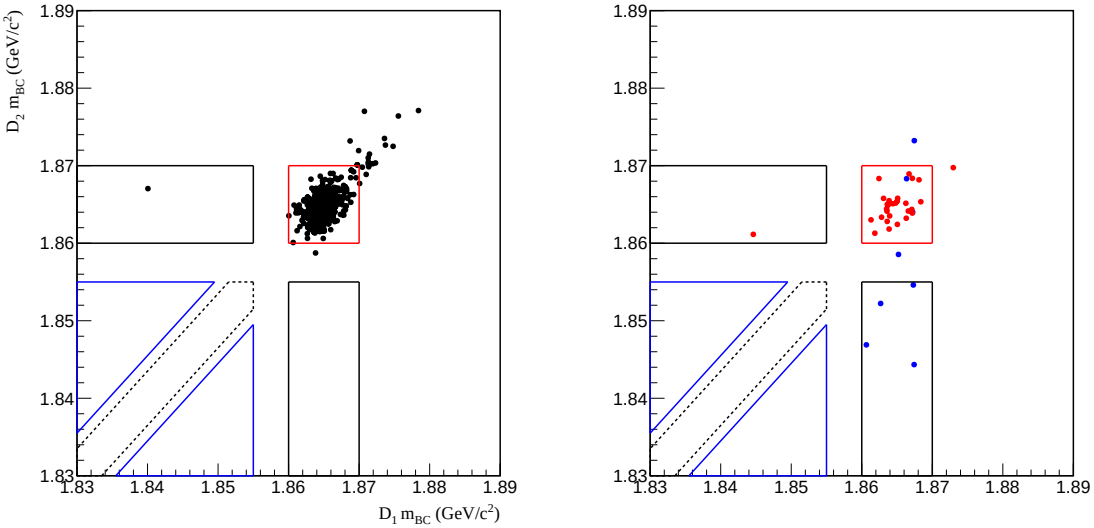

Figure 13: $m_{\rm BC}$ plane in generic MC for $4\pi^{\pm}$ tagged with $\pi^+\pi^-$. The left plot shows signal candidates, the right plot shows background candidates. The red points are the peaking $K^0_S\pi^+\pi^-$ vs $\pi^+\pi^-$ background and the blue points are all other backgrounds.

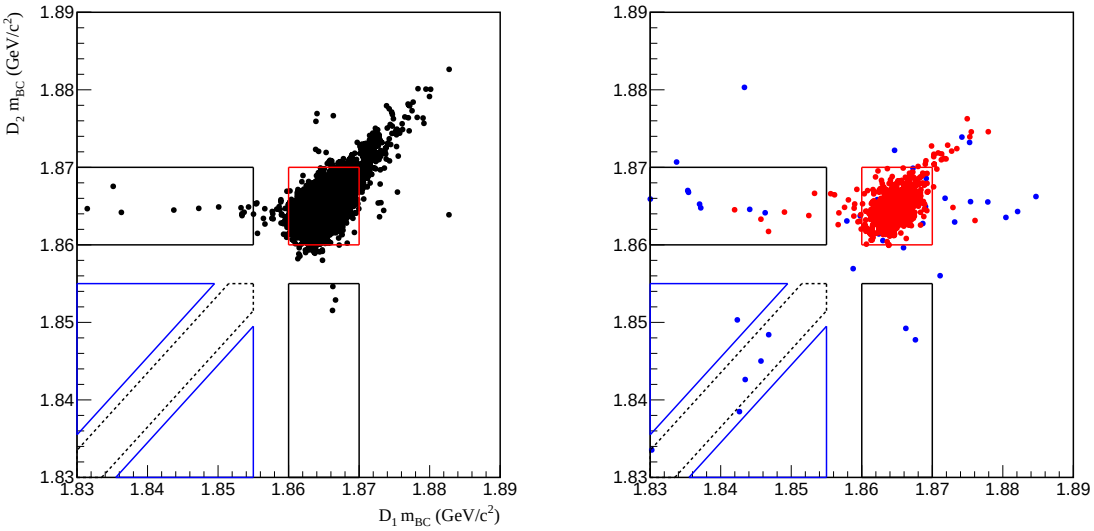

Figure 14: $m_{\rm BC}$ plane in generic MC for $4\pi^{\pm}$ tagged with $K^{\pm}\pi^{\mp}$. The left plot shows signal candidates, the right plot shows background candidates. The red points are the peaking $K^0_S\pi^+\pi^-$ vs $K^{\pm}\pi^{\mp}$ background and the blue points are all other backgrounds.

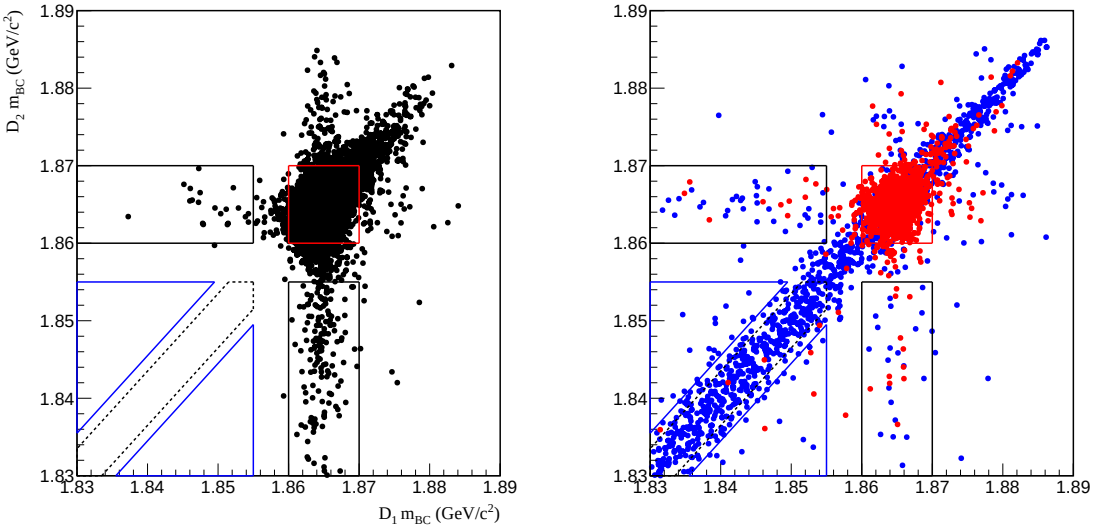

Figure 15: $m_{\rm BC}$ plane in generic MC for $4\pi^{\pm}$ tagged with $K^{\pm}\pi^{\mp}\pi^{0}$. The left plot shows signal candidates, the right plot shows background candidates. The red points are the peaking $K^{0}_{S}\pi^{+}\pi^{-}$ vs $K^{\pm}\pi^{\mp}\pi^{0}$ background and the blue points are all other backgrounds.

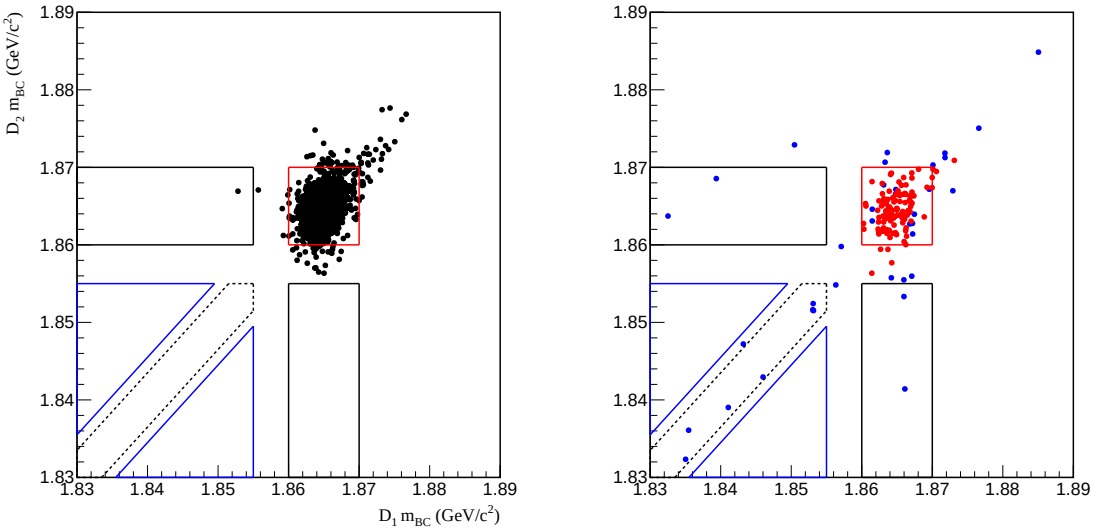

Figure 16: $m_{\rm BC}$ plane in generic MC for $4\pi^{\pm}$ tagged with $K^{0}_{S}\pi^{0}$. The left plot shows signal candidates, the right plot shows background candidates. The red points are the peaking $K^{0}_{S}\pi^{+}\pi^{-}$ vs $K^{0}_{S}\pi^{0}$ background and the blue points are all other backgrounds.

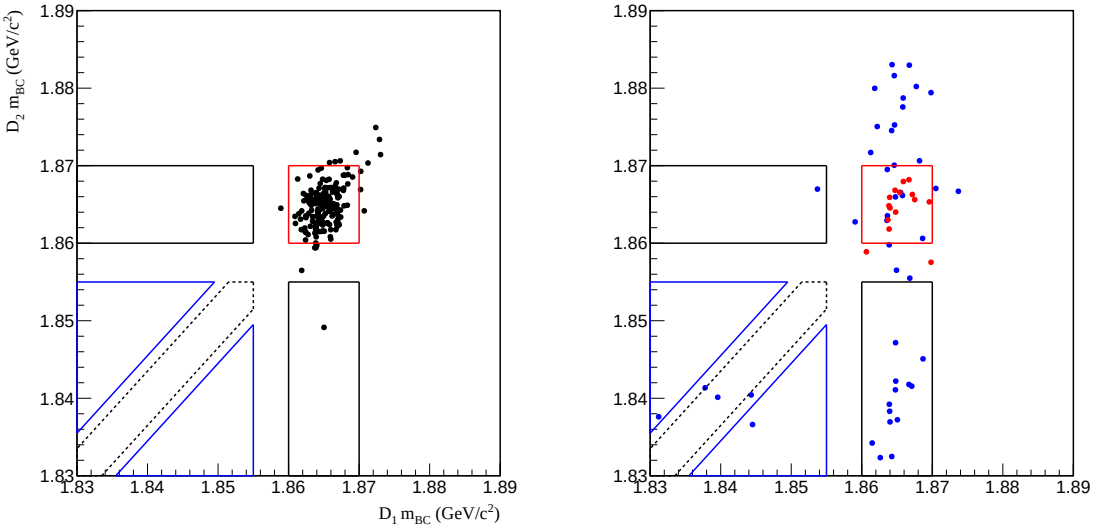

Figure 17: $m_{\rm BC}$ plane in generic MC for $4\pi^{\pm}$ tagged with $K^0_S\eta$. The left plot shows signal candidates, the right plot shows background candidates. The red points are the peaking $K^0_S\pi^+\pi^-$ vs $K^0_S\eta$ background and the blue points are all other backgrounds.

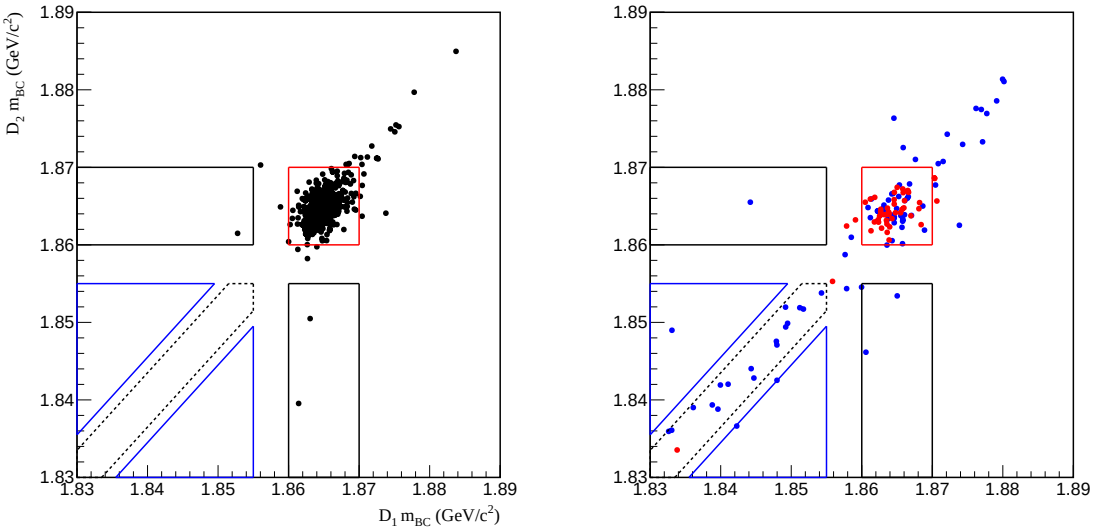

Figure 18: $m_{\rm BC}$ plane in generic MC for $4\pi^{\pm}$ tagged with $K^0_S\omega$. The left plot shows signal candidates, the right plot shows background candidates. The red points are the peaking $K^0_S\pi^+\pi^-$ vs $K^0_S\omega$ background and the blue points are all other backgrounds.

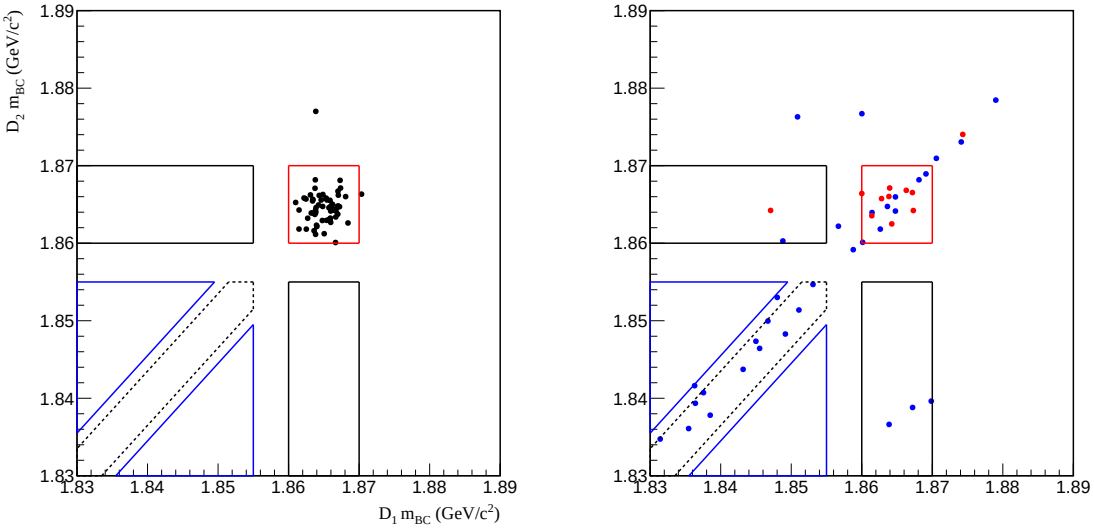

Figure 19: $m_{\rm BC}$ plane in generic MC for $4\pi^{\pm}$ tagged with $K^0_S\eta(\pi^+\pi^-\pi^0)$. The left plot shows signal candidates, the right plot shows background candidates. The red points are the peaking $K^0_S\pi^+\pi^-$ vs $K^0_S\eta(\pi^+\pi^-\pi^0)$ background and the blue points are all other backgrounds.

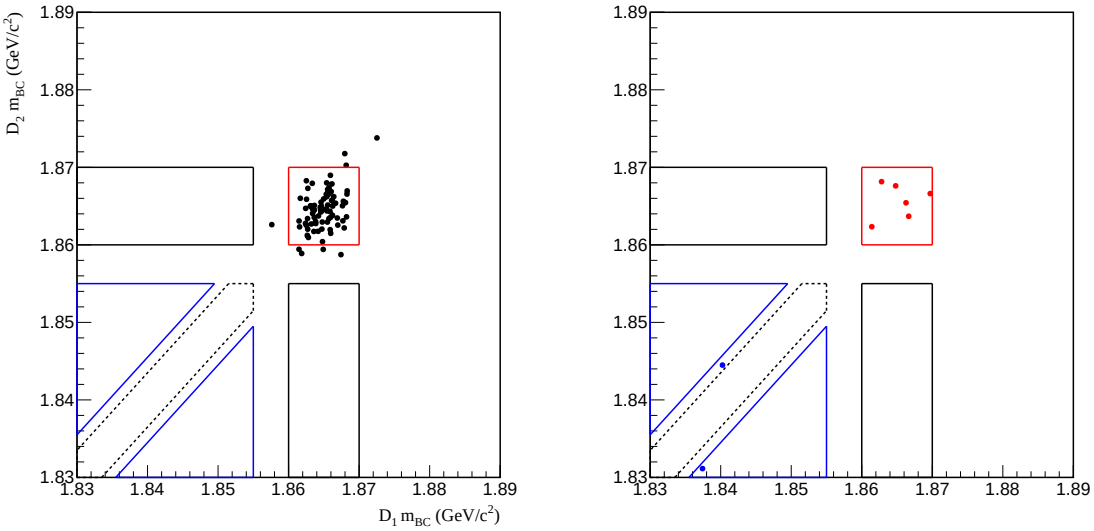

Figure 20: $m_{\rm BC}$ plane in generic MC for $4\pi^{\pm}$ tagged with $K^0_S\eta'(\pi^+\pi^-\eta)$. The left plot shows signal candidates, the right plot shows background candidates. The red points are the peaking $K^0_S\pi^+\pi^-$ vs $K^0_S\eta'(\pi^+\pi^-\eta)$ background and the blue points are all other backgrounds.

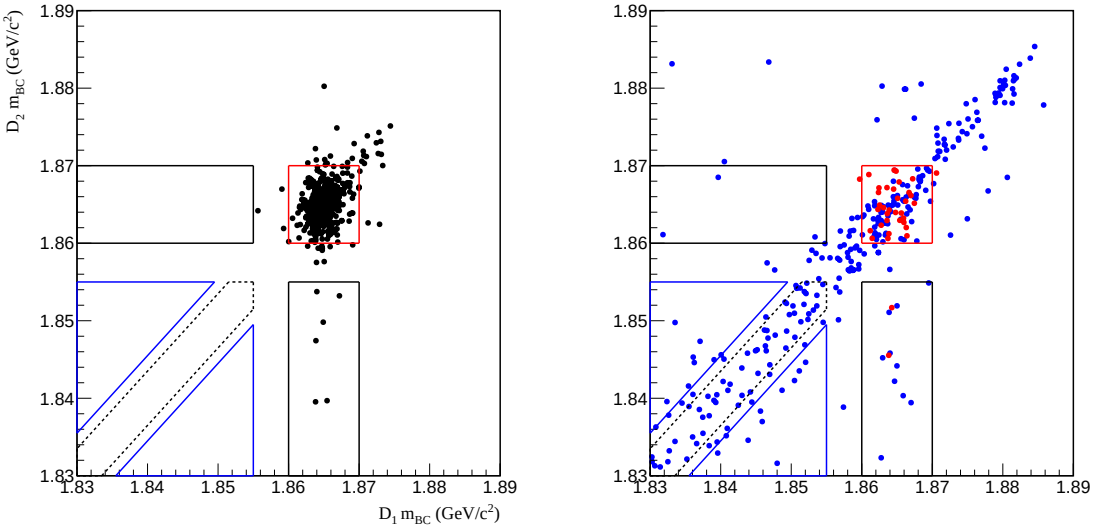

Figure 21: $m_{\rm BC}$ plane in generic MC for $4\pi^{\pm}$ tagged with $K^0_S\pi^0\pi^0$. The left plot shows signal candidates, the right plot shows background candidates. The red points are the peaking $K^0_S\pi^+\pi^-$ vs $K^0_S\pi^0\pi^0$ background and the blue points are all other backgrounds.

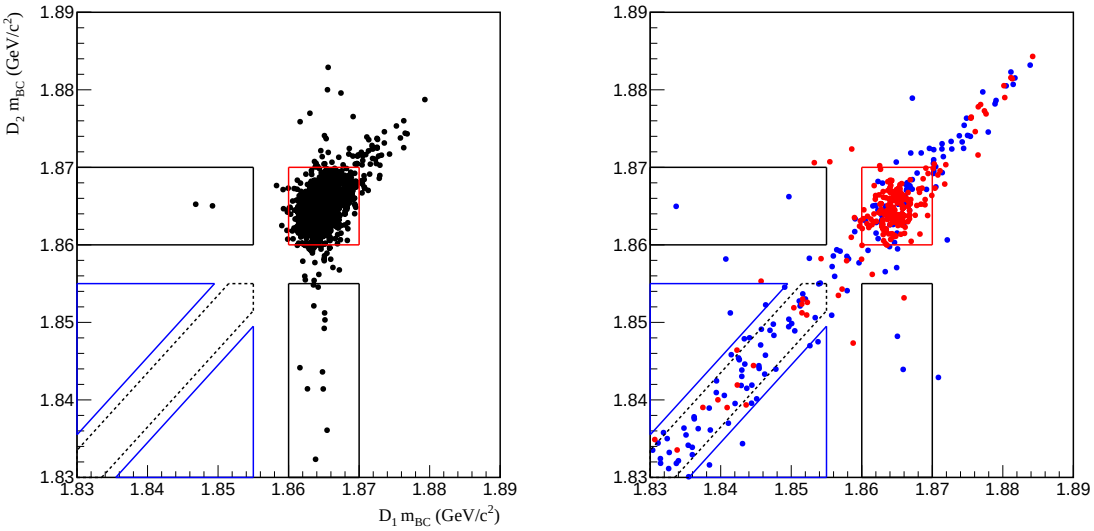

Figure 22: $m_{\rm BC}$ plane in generic MC for $4\pi^{\pm}$ tagged with $\pi^+\pi^-\pi^0$. The left plot shows signal candidates, the right plot shows background candidates. The red points are the peaking $K^0_S\pi^+\pi^-$ vs $\pi^+\pi^-\pi^0$ background and the blue points are all other backgrounds.

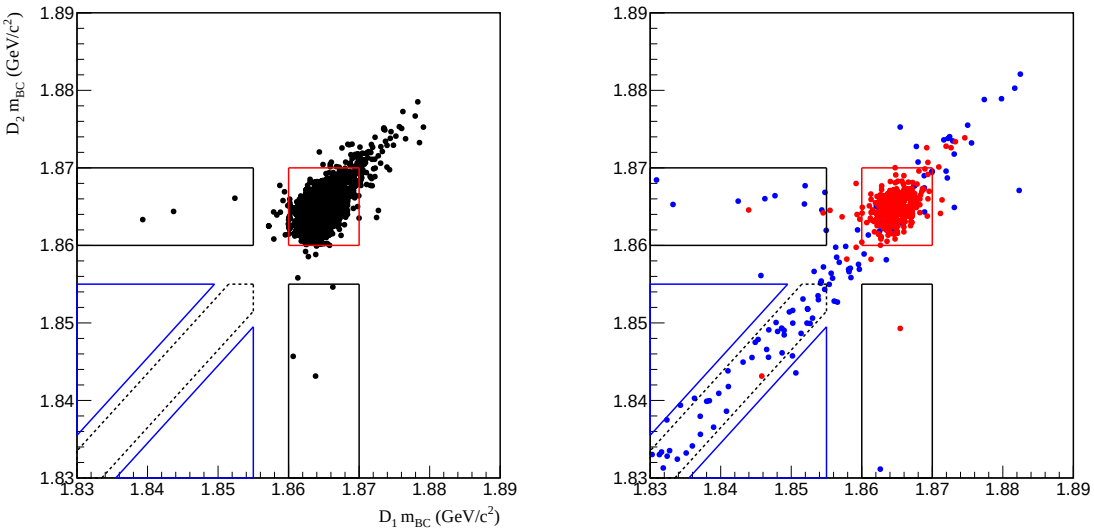

Figure 23: $m_{\rm BC}$ plane in generic MC for $4\pi^{\pm}$ tagged with $K^0_S\pi^+\pi^-$. The left plot shows signal candidates, the right plot shows background candidates. The red points are the peaking $K^0_S\pi^+\pi^-$ vs $K^0_S\pi^+\pi^-$ background and the blue points are all other backgrounds.

2.8 Continuum MC $m_{\rm BC}$ planes

Figures 25 and 26 show the distribution of the continuum-dominated double-tags on the $m_{\rm BC}$ plane in continuum MC.

2.9 Data Dalitz plots

Example Dalitz plots in data are shown for $4\pi^{\pm}$ tagged with $K^{\pm}\pi^{\mp}\pi^0$ in Figures 27–31. The pions labelled 1 and 2 (3 and 4) have positive (negative) charge. At present no randomisation is applied to the same-sign pions.

2.10 Results for modes without continuum dominance

To determine the number of signal candidates, the flat and peaking background estimates are subtracted from the total yield in the signal region. Peaking backgrounds are assumed to be entirely due to $K^0_S\pi^+\pi^-$ vs tag (and $K^0_S\pi^+\pi^-$ vs $K^0_S\pi^+\pi^-$ for $4\pi^{\pm}$ vs $4\pi^{\pm}$). The yield of this background in MC, $B_{\rm peak}$, is determined as follows:

$$B_{\rm peak} = n^{31-37}_{\rm peak} \times f^{31-37} + n^{43-46}_{\rm peak} \times f^{43-46} \quad (1)$$

where the MC-data scaling factors $f^{31-37} = 0.105$, $f^{43-46} = 0.05$ and $n^{x-y}_{\rm peak}$ refer to the yields in the run range x–y. The signal and background yields are shown in Table 7. The numbers for the four continuum-dominated modes are not shown; for those see Section 2.11. The factor of four between the two peaking samples makes sense. There is twice as much data in datasets 43–46, and twice as much MC was generated.

2.11 Results for modes with continuum dominance

Modes with significant contributions from continuum decays are considered using two approaches.

2.11.1 Method 1: naive MC scaling

The quantities of continuum MC in the signal region and sideband C are scaled by the factor 0.581 discussed previously. The amount in the signal region, $B_{\rm cont}$, is treated as another peaking background and subtracted off the raw data yield. The amount in sideband C is subtracted from the amount in data prior to the usual

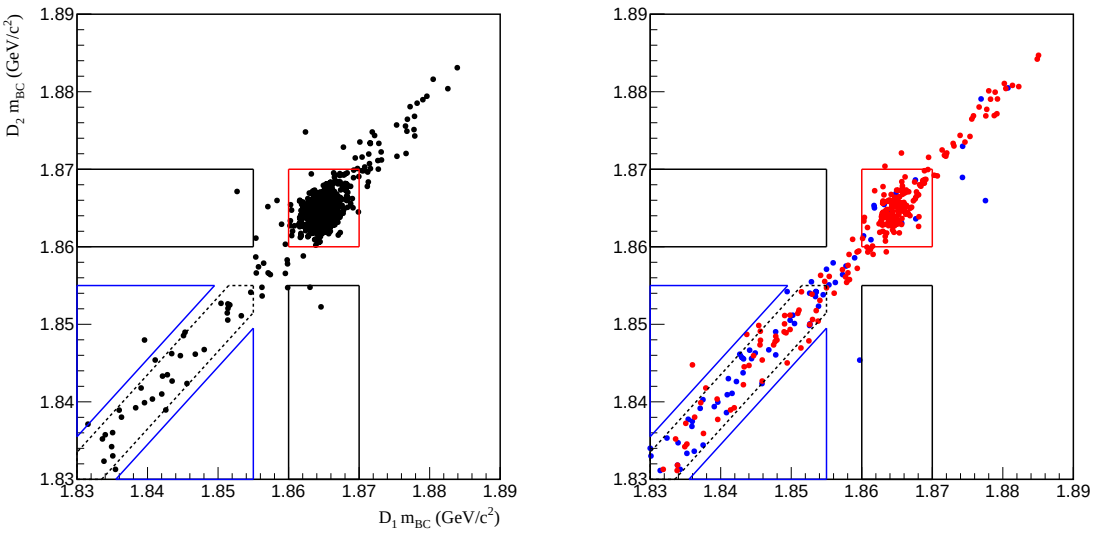

Figure 24: $m_{\rm BC}$ plane in generic MC for $4\pi^{\pm}$ tagged with $4\pi^{\pm}$. The left plot shows signal candidates, the right plot shows background candidates. The red points are the peaking $K^0_S\pi^+\pi^-$ vs ($4\pi^{\pm}$ or $K^0_S\pi^+\pi^-$) background and the blue points are all other backgrounds.

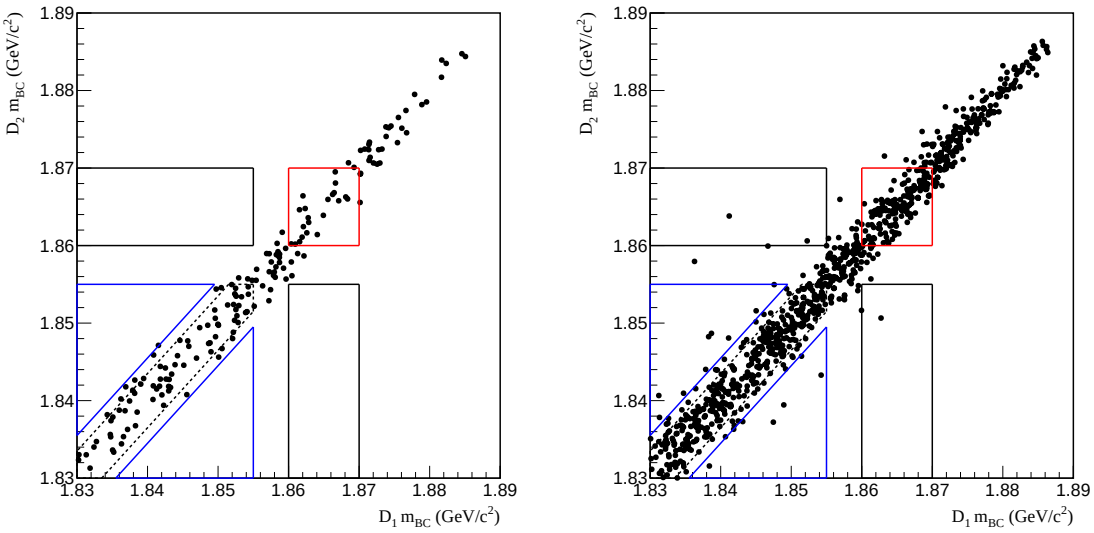

Figure 25: $m_{\rm BC}$ plane in continuum MC for $4\pi^{\pm}$ tagged with (left) K^+K^- (right) $\pi^+\pi^-$.

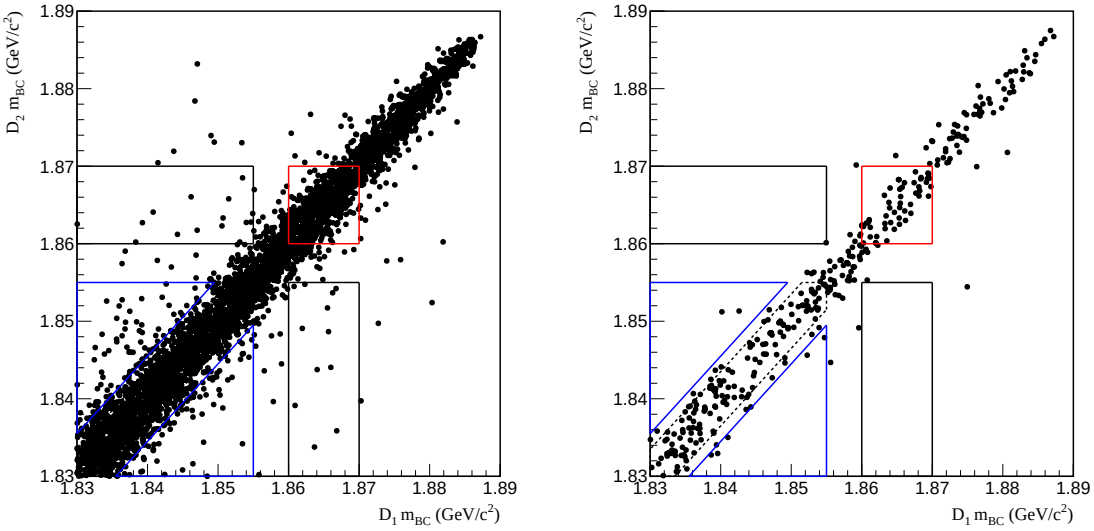

Figure 26: $m_{\rm BC}$ plane in continuum MC for $4\pi^{\pm}$ tagged with (left) $\pi^+\pi^-\pi^0$ (right) $4\pi^{\pm}$.

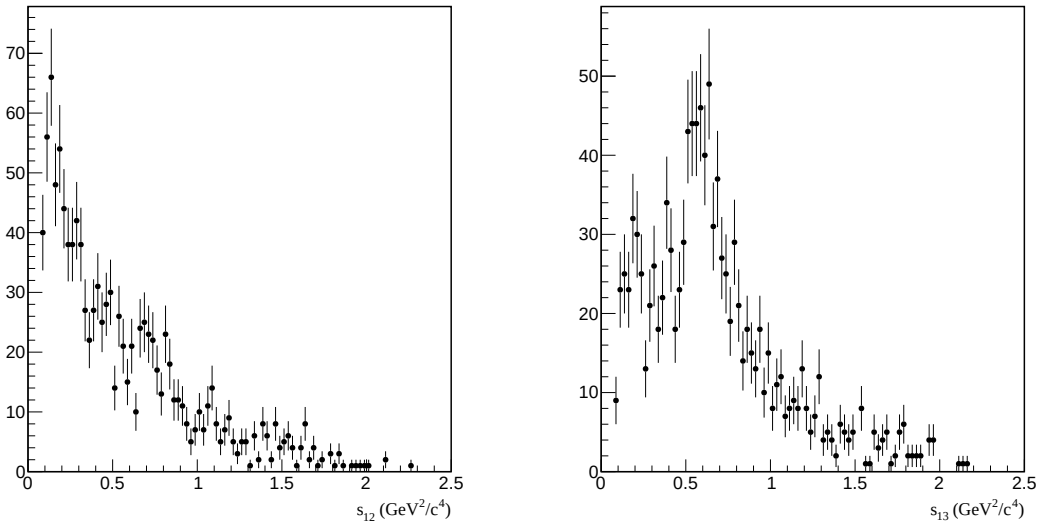

Figure 27: Dalitz plot variables s_{12} and s_{13} for $4\pi^{\pm}$ tagged with $K^{\pm}\pi^{\mp}\pi^0$ in data.

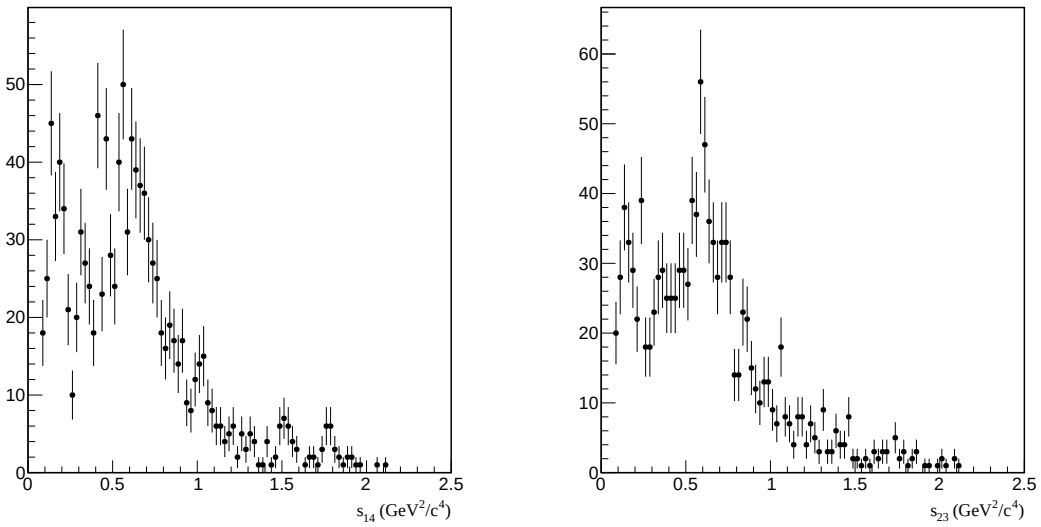

Figure 28: Dalitz plot variables s_{14} and s_{23} for $4\pi^{\pm}$ tagged with $K^{\pm}\pi^{\mp}\pi^0$ in data.

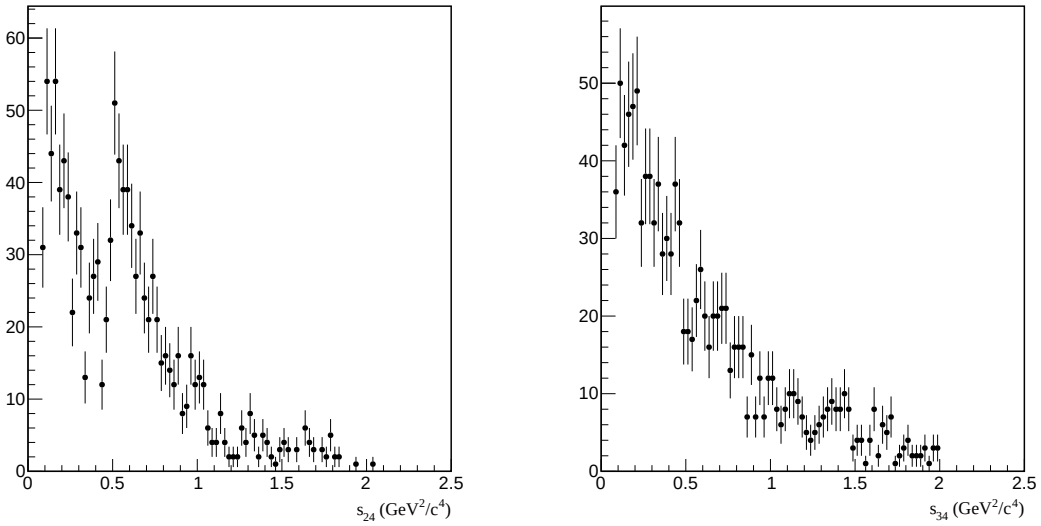

Figure 29: Dalitz plot variables s_{24} and s_{34} for $4\pi^{\pm}$ tagged with $K^{\pm}\pi^{\mp}\pi^0$ in data.

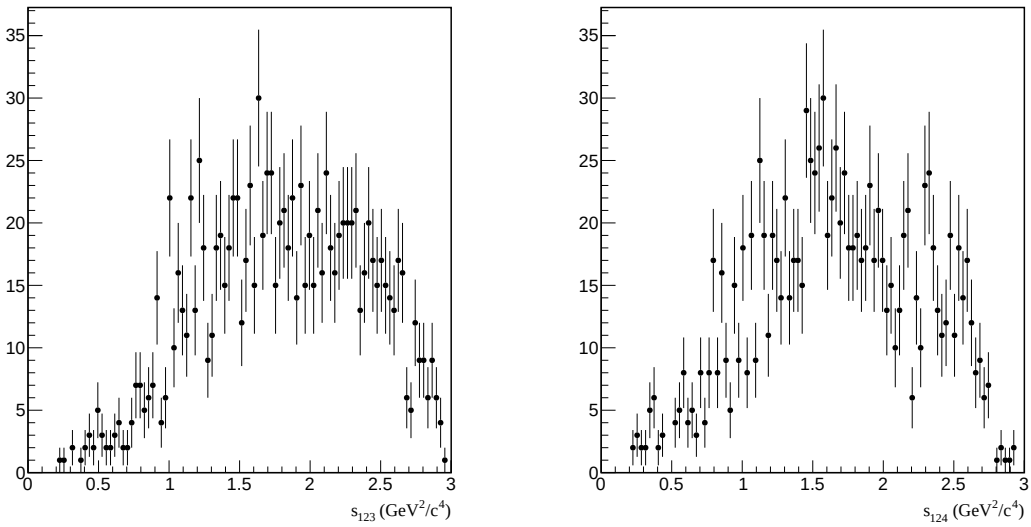

Figure 30: Dalitz plot variables s_{123} and s_{124} for $4\pi^{\pm}$ tagged with $K^{\pm}\pi^{\mp}\pi^0$ in data.

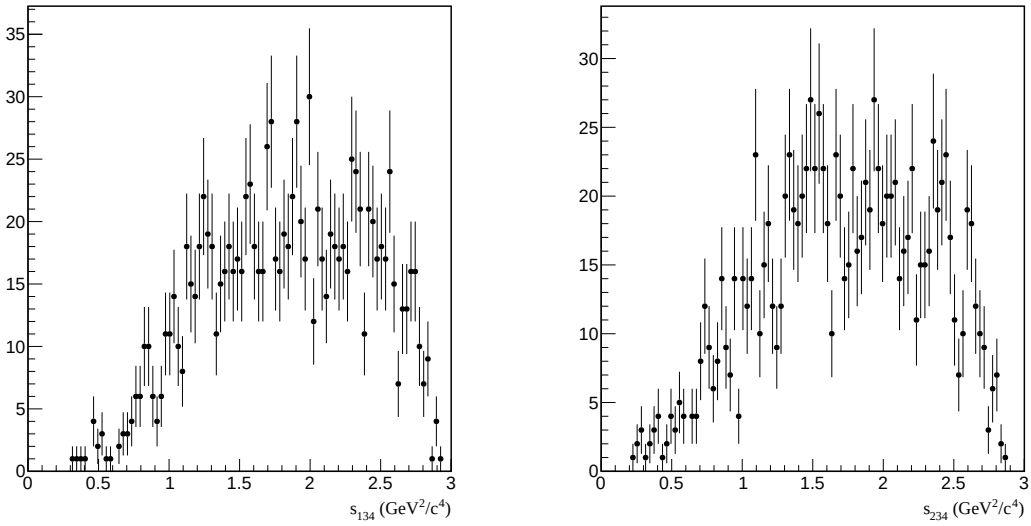

Figure 31: Dalitz plot variables s_{134} and s_{234} for $4\pi^{\pm}$ tagged with $K^{\pm}\pi^{\mp}\pi^0$ in data.

Decay mode	Total S-box yield	$B_{\rm flat}$	$n_{\rm peak}$		$B_{\rm peak}$	Signal
			31–37	43–46		
$K^\pm\pi^\mp$	600	4.4 ± 1.7	160	585	46.0 ± 1.8	549.6 ± 24.8
$K^0_S\pi^0$	120	1.0 ± 0.6	19	83	6.1 ± 0.6	112.8 ± 11.0
$K^0_S\eta(\gamma\gamma)$	20	0.4 ± 0.4	3	10	0.8 ± 0.2	18.8 ± 4.5
$K^0_S\omega$	44	0.6 ± 0.6	8	31	2.4 ± 0.4	41.0 ± 6.7
$K^0_S\eta(\pi^+\pi^-\pi^0)$	7	0.0	14	48	3.9 ± 0.5	3.1 ± 2.7
$K^0_S\eta'(\pi^+\pi^-\eta)$	10	0.4 ± 0.4	1	4	0.3 ± 0.2	9.3 ± 3.2
$K^0_S\pi^0\pi^0$	23	2.4 ± 1.6	7	25	2.0 ± 0.4	18.6 ± 5.1
$K^\pm\pi^\mp\pi^0$	1223	25.4 ± 4.6	300	1356	99.3 ± 2.6	1098.3 ± 35.0
$K^0_S\pi^+\pi^-$	248	11.6 ± 2.9	63	263	19.8 ± 1.2	216.6 ± 16.0

Table 7: Signal and background yields in the signal region for modes that are not continuum-dominated.

flat background calculation. Results are shown in Table 8. Considering that there are several significantly negative yields is clear that this method is unreliable. (The values for K^+K^- and $\pi^+\pi^-$ are very close to those obtained in Method 2, however.)

Decay mode	Total S-box yield	$B_{\rm cont}$		$n_{\rm peak}$		$B_{\rm peak}$	$B_{\rm flat}$	Signal
		S	C	31–37	43–46			
K^+K^-	34	13.9	43.6	14	43	3.6 ± 0.5	-3.1 ± 4.9	19.5 ± 8.1
$\pi^+\pi^-$	83	83.7	203.3	8	19	1.8 ± 0.4	-4.9 ± 11.2	2.4 ± 16.2
$\pi^+\pi^-\pi^0$	188	450.9	1112.0	90	375	28.2 ± 1.4	-567.7 ± 18.4	276.7 ± 28.0
$4\pi^\pm$ (K^0_S FS < 0)	344	29.6	79.0	27	106	8.1 ± 0.8	429.7 ± 18.5	-123.4 ± 26.5
$4\pi^\pm$ (K^0_S FS < -2)	257	23.8	61.6	12	38	3.2 ± 0.5	328.3 ± 16.3	-98.3 ± 23.5
$4\pi^\pm$ (K^0_S mass veto)	386	37.2	93.5	24	79	6.5 ± 0.7	484.4 ± 19.6	-142.1 ± 28.0

Table 8: Signal and background yields in the signal region for modes that are continuum-dominated, using naive scaling. **These numbers should not be used.**

2.11.2 Method 2: fit to average $m_{\rm BC}$

The average value of $m_{\rm BC}$ of the two final states is used to determine the quantity of signal MC. This method was used in the $h^+h^-\pi^0$ paper. The difference here is the significant quantity of $K^0_S\pi^+\pi^-$ peaking background that remains even after the K^0_S veto.

The signal and peaking background components are both parameterised with the sum of two Crystal Ball functions. The shape parameters are the common mean μ, the common width σ, the relative fraction f and the tail parameters $\alpha_{L,R}$ and $n_{L,R}$. The values of $n_{L,R}$ are fixed at 3; there are not enough events to float them. In the (current) absence of signal MC samples the generic MC sample is used to determine the parameters in each case. Figures 32 and 33 show the fits to signal MC.

There are three components in the fit to data: signal, peaking background and continuum/flat backgroud. The signal shape parameters are fixed to the values found in MC. The peaking background is determined from a fit to $K^0_S\pi^+\pi^-$ tagged with the relevant final state in each case. The continuum/flat background is parameterised with an ARGUS function whose parameters, except the threshold, are floating. The yield of the peaking background is fixed to the value scaled from MC, i.e. $B_{\rm peak}$. The yield of the signal and continuum/flat background are floating. Figures 34 and 35 show the fits to data.

The signal candidate yields are:

- K^+K^-: 19.4 ± 6.3

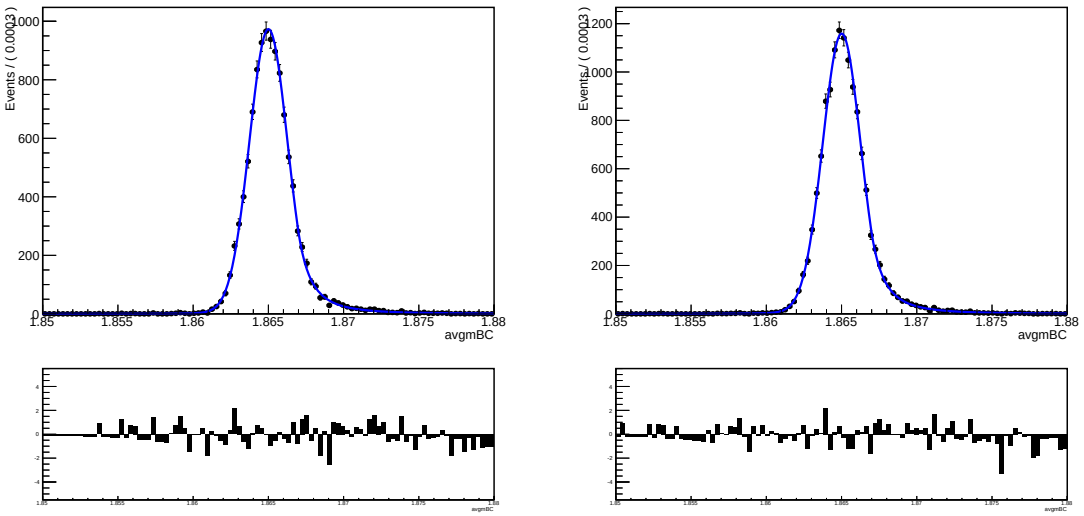

Figure 32: Fit to generic MC signal for $4\pi^{\pm}$ tagged with (left) K^+K^- (right) $\pi^+\pi^-$.

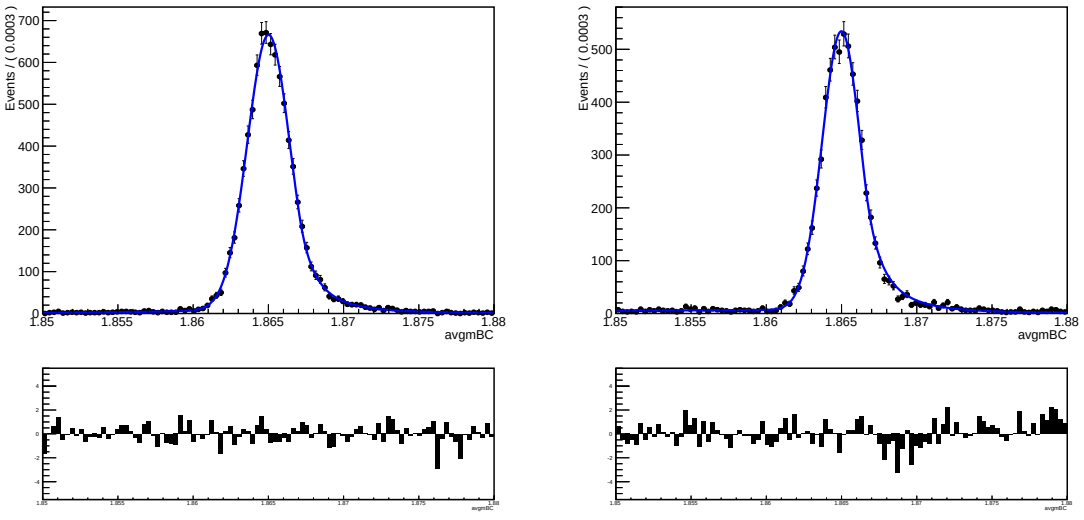

Figure 33: Fit to generic MC signal for $4\pi^{\pm}$ tagged with (left) $\pi^+\pi^-\pi^0$ (right) $4\pi^{\pm}$.

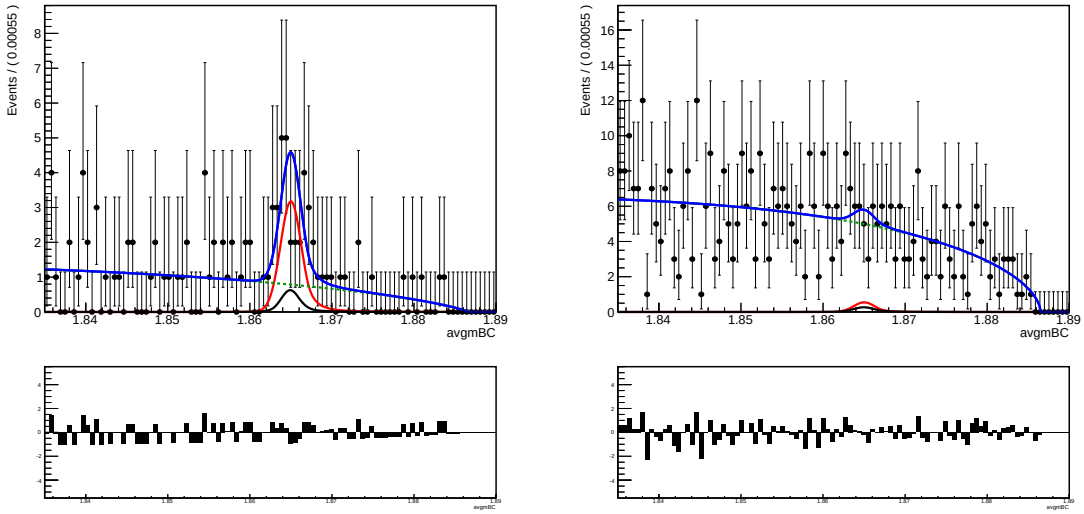

Figure 34: Fit to data for $4\pi^{\pm}$ tagged with (left) K^+K^- (right) $\pi^+\pi^-$. The blue curve is the total PDF, the red curve is the signal, the black curve is the peaking background and the dashed green curve is the continuum/flat background.

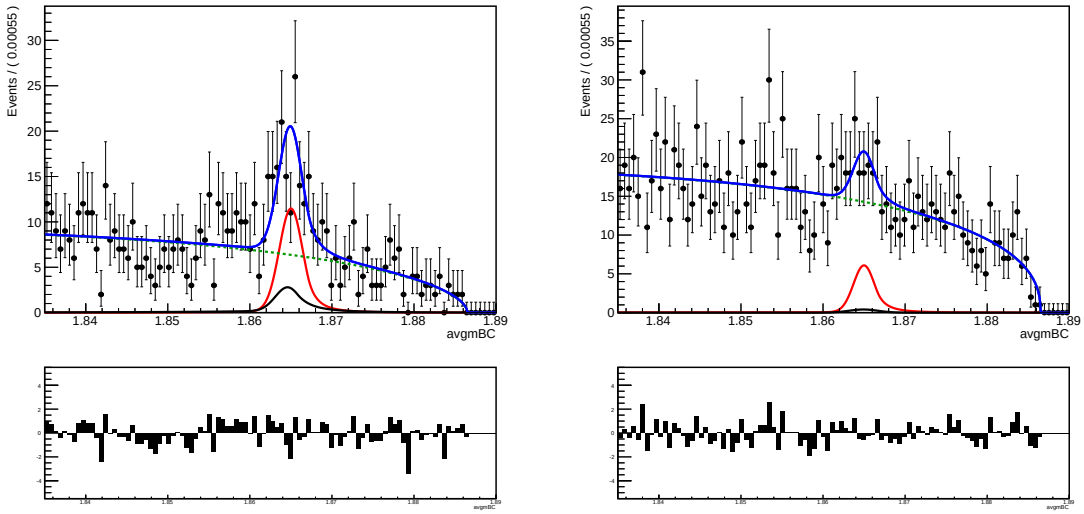

Figure 35: Fit to data for $4\pi^{\pm}$ tagged with (left) $\pi^+\pi^-\pi^0$ (right) $4\pi^{\pm}$. The blue curve is the total PDF, the red curve is the signal, the black curve is the peaking background and the dashed green curve is the continuum/flat background.

- $\pi^+\pi^-$: 3.3 ± 8.2
- $\pi^+\pi^-\pi^0$: 81.4 ± 15.2
- $4\pi^\pm$ (K_S^0 FS < 0): 68.6 ± 18.6
- $4\pi^\pm$ (K_S^0 FS < -2): 41.0 ± 16.3
- $4\pi^\pm$ (K_S^0 mass veto): 63.0 ± 19.3

3 Partially-reconstructed selection results

3.1 Data yields

The number of candidates selected in data for each partially-reconstructed decay mode at different selection stages is shown in Table 9.

Decay mode	DTag		Cuts		K^0_S veto	On $m^2_{\rm miss}$ projection		
	Cands.	Events	Cands.	Events	and MCS	L	S	H
$K^0_L\pi^0$	40681	22928	234	205	100	13	75	5
$K^0_L\omega$	260740	126181	149	123	77	8	33	27
$K^0_L\pi^+\pi^-$	142532	94828	3371	2878	1742	433	601	257

Table 9: Candidate and event yields in partially-reconstructed data at various stages: '`DTag`' is number from `DTag` software, 'Cuts' is number after selection cuts, 'K^0_S veto and MCS' is number after K^0_S veto and multiple candidate selection have been applied. 'On $m^2_{\rm miss}$ projection indicates number of candidates in each region on the $m^2_{\rm miss}$ projection (Low, Signal, High).

3.2 Generic MC yields

The number of candidates selected in MC for each partially-reconstructed decay mode at different selection stages is shown in Table 10.

Decay mode	DTag		Cuts		K^0_S veto	On $m^2_{\rm miss}$ projection								
	Cands.	Events	Cands.	Events	and MCS	L			S			H		
						Sig	Peak	Other	Sig	Peak	Other	Sig	Peak	Other
$K^0_L\pi^0$	122514	85397	4481	4481	2063	2	0	38	1676	157	49	2	2	81
$K^0_L\omega$	420167	237692	1962	1951	916	0	0	6	563	61	38	4	9	210
$K^0_L\pi^+\pi^-$	363890	270205	34257	33757	16156	25	24	3027	6117	793	393	85	32	2328

Table 10: Candidate and event yields in partially-reconstructed generic MC at various stages: '`DTag`' is number from `DTag` software, 'Cuts' is number after selection cuts, 'K^0_S veto and MCS' is number after K^0_S veto and multiple candidate selection have been applied. 'On $m^2_{\rm miss}$ projection indicates number of candidates in each region on the $m^2_{\rm miss}$ projection (Low, Signal, High). 'Sig' is the number of truth-matched $4\pi^\pm$ vs tag candidates, 'Peak' is the number of peaking background candidates, and 'Other' encompasses all remaining background candidates.

3.3 Continuum MC yields

The number of candidates selected in MC for each partially-reconstructed decay mode at different selection stages is shown in Table 11.

3.4 Signal MC

Signal efficiencies for partially-reconstructed modes are listed in Table 12. The events are required to lie in the $m_{\rm BC}$ vs $m^2_{\rm miss}$ signal region. Efficiencies are determined with respect to the number at generator level. The efficiencies of the equivalent $K^0_S\pi^+\pi^-$ peaking backgrounds are also shown.

The two-dimensional K^0_L shower cut described in Section 1.6 is removed and the efficiencies are recalculated. Results are shown in Table 13.

Decay mode	DTag		Cuts		K^0_S veto	On $m^2_{\rm miss}$ projection		
	Cands.	Events	Cands.	Events	and MCS	L	S	H
$K^0_L\pi^0$	60566	39060	97	97	73	24	31	5
$K^0_L\omega$	370618	214733	65	65	53	11	7	19
$K^0_L\pi^+\pi^-$	169783	136527	1937	1928	1600	849	122	123

Table 11: Candidate and event yields in partially-reconstructed continuum MC at various stages: '`DTag`' is number from `DTag` software, 'Cuts' is number after selection cuts, 'K^0_S veto and MCS' is number after K^0_S veto and multiple candidate selection have been applied. 'On $m^2_{\rm miss}$ projection indicates number of candidates in each region on the $m^2_{\rm miss}$ projection (Low, Signal, High).

Decay mode	Reconstructed as	Efficiency at gen. level (%)
$4\pi^\pm$ vs $K^0_L\pi^0$	Itself	19.8 ± 0.2
$4\pi^\pm$ vs $K^0_L\omega$	Itself	7.5 ± 0.1
$4\pi^\pm$ vs $K^0_L\pi^+\pi^-$	Itself	30.1 ± 0.2
$K^0_S\pi^+\pi^-$ vs $K^0_L\pi^0$	$4\pi^\pm$ vs $K^0_L\pi^0$	0.3 ± 0.0
$K^0_S\pi^+\pi^-$ vs $K^0_L\omega$	$4\pi^\pm$ vs $K^0_L\omega$	0.2 ± 0.0
$K^0_S\pi^+\pi^-$ vs $K^0_L\pi^+\pi^-$	$4\pi^\pm$ vs $K^0_L\pi^+\pi^-$	0.5 ± 0.0

Table 12: Signal MC efficiencies for partially-reconstructed decay modes.

Decay mode	Reconstructed as	Efficiency at gen. level (%)
$4\pi^\pm$ vs $K^0_L\pi^0$	Itself	21.3 ± 0.2
$4\pi^\pm$ vs $K^0_L\omega$	Itself	8.4 ± 0.1
$4\pi^\pm$ vs $K^0_L\pi^+\pi^-$	Itself	33.9 ± 0.2

Table 13: Signal MC efficiencies for partially-reconstructed decay modes without applying the K^0_L shower cut.

3.5 Data m^2_{miss} projections

Figures 36 and 37 show the distribution of each partially-reconstructed tag on the m^2_{miss} projection in data.

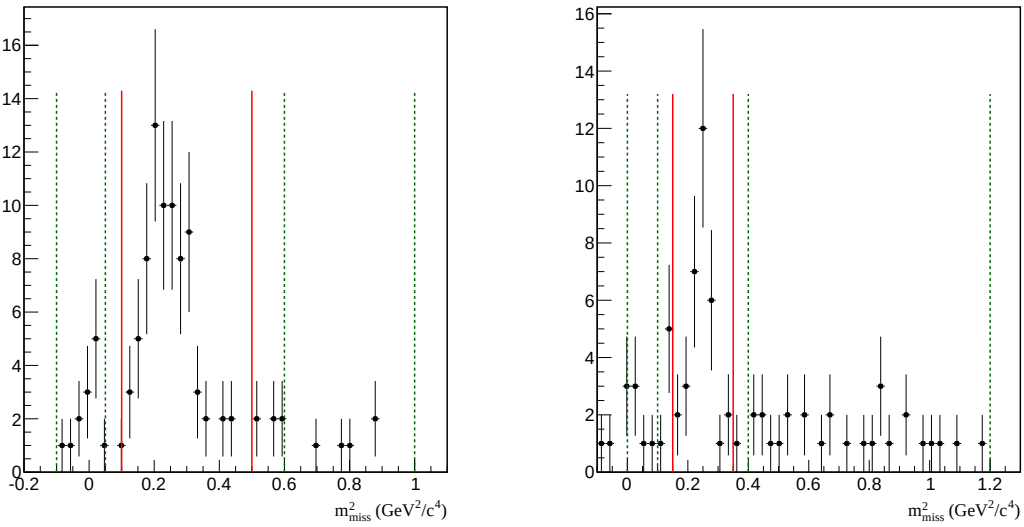

Figure 36: m^2_{miss} projection for $4\pi^{\pm}$ tagged with (left) $K^0_L\pi^0$ (right) $K^0_L\omega$. The red lines indicate the signal region and the two sets of dashed green lines indicate the low and high sidebands.

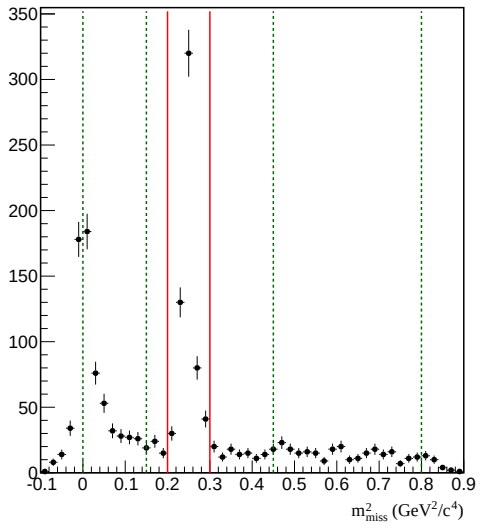

Figure 37: m^2_{miss} projection for $4\pi^{\pm}$ tagged with $K^0_L\pi^+\pi^-$. The red lines indicate the signal region and the two sets of dashed green lines indicate the low and high sidebands.

3.6 Generic MC m^2_{miss} projections

Figures 38 and 39 show the distribution of each partially-reconstructed tag on the m^2_{miss} projection in generic MC.

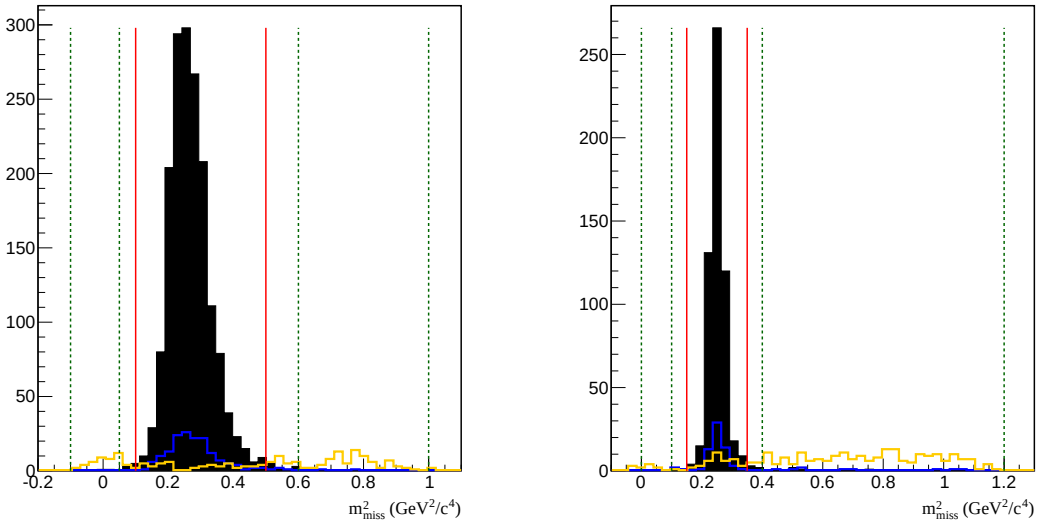

Figure 38: m^2_{miss} projection for $4\pi^{\pm}$ tagged with (left) $K^0_L\pi^0$ (right) $K^0_L\omega$ in generic MC. The solid black histogram is MC signal, the open blue histogram is the peaking background and the open orange histogram is the non-peaking background. The red lines indicate the signal region and the two sets of dashed green lines indicate the low and high sidebands.

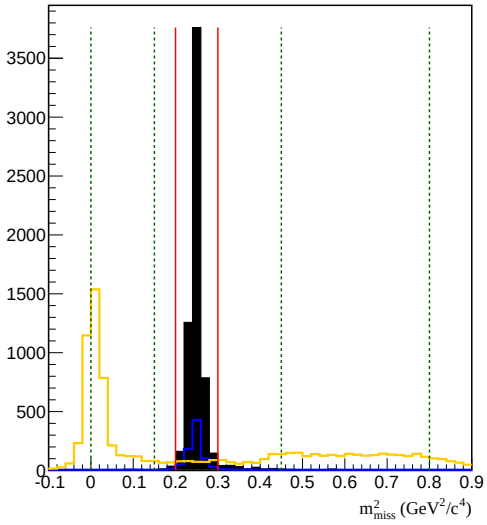

Figure 39: m^2_{miss} projection for $4\pi^{\pm}$ tagged with $K^0_L\pi^+\pi^-$ in generic MC. The solid black histogram is MC signal, the open blue histogram is the peaking background and the open orange histogram is the non-peaking background. The red lines indicate the signal region and the two sets of dashed green lines indicate the low and high sidebands.

3.7 Continuum MC $m^2_{\rm miss}$ projections

Figures 40 and 41 show the distribution of each partially-reconstructed tag on the $m^2_{\rm miss}$ projection in continuum MC. There is a peak around $m^2_{\rm miss} = 0$ for all modes. The contribution to $K^0_L\pi^+\pi^-$ is particularly large.

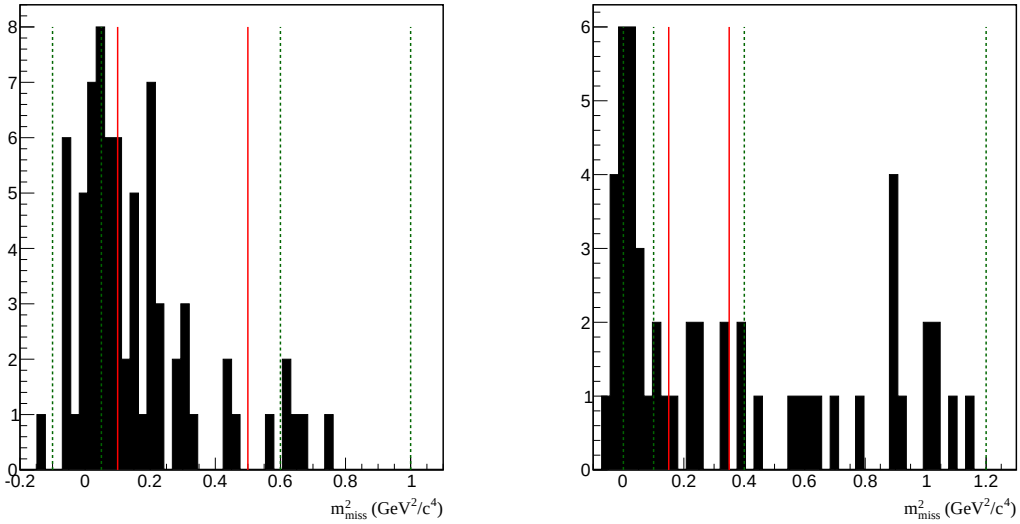

Figure 40: $m^2_{\rm miss}$ projection for $4\pi^\pm$ tagged with (left) $K^0_L\pi^0$ (right) $K^0_L\omega$ in continuum MC. The red lines indicate the signal region and the two sets of dashed green lines indicate the low and high sidebands.

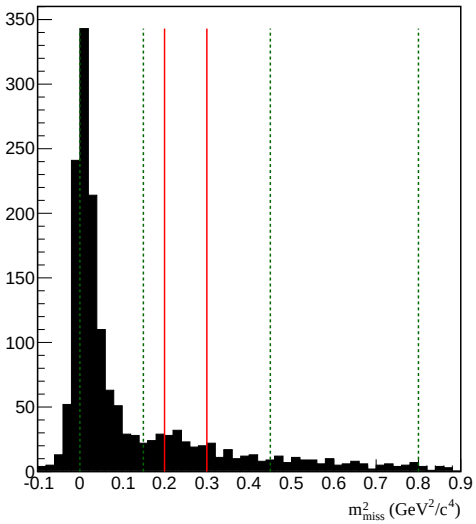

Figure 41: $m^2_{\rm miss}$ projection for $4\pi^\pm$ tagged with $K^0_L\pi^+\pi^-$ in continuum MC. The red lines indicate the signal region and the two sets of dashed green lines indicate the low and high sidebands.

3.8 Results

The MC studies have revealed that there are several sources of background to the partially-reconstructed modes: peaking, continuum and various other misidentified decays.

The same background subtraction as used for $h^+h^-\pi^0$ vs $K^0_L\pi^+\pi^-$ is employed. The results of this procedure are shown in Table 14. By construction the sum of the signal and background yields is equal to

Mode	Signal	Peaking background	Non-peaking background	Continuum background
$K^0_L\pi^0$	49.2 ± 10.9	9.1 ± 0.8	1.5 ± 1.8	15.2 ± 7.2
$K^0_L\omega$	22.0 ± 6.5	3.7 ± 0.5	2.5 ± 1.7	4.8 ± 3.3

Table 14: Signal and background yields in the signal region.

the number of events in the signal region.

Overlays of the scaled MC samples with the data for each mode are shown in Figure 42. Good agreement is observed.

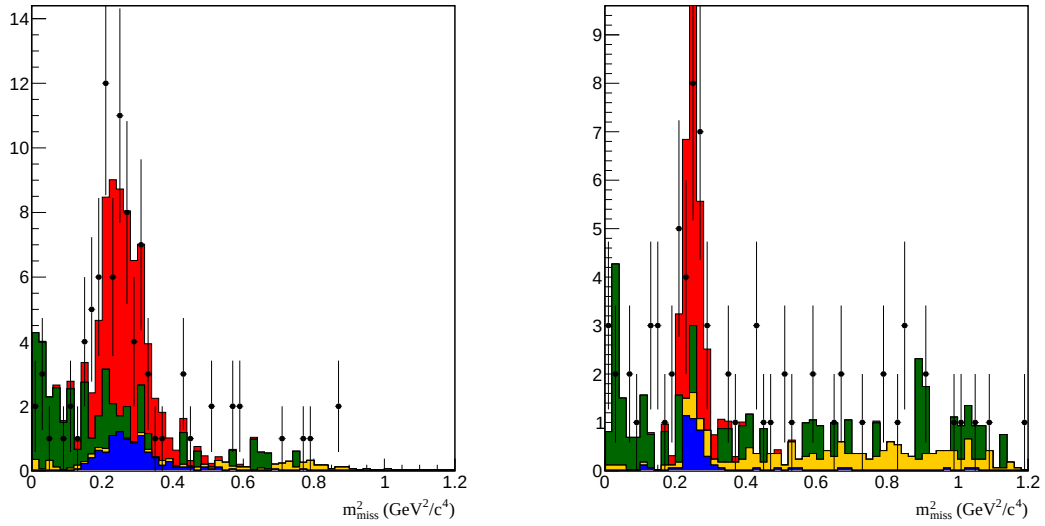

Figure 42: Comparison of $m^2_{\rm miss}$ distribution of data (black points) with various sources of MC which have been scaled to the expected yields as found in the background subtraction method. The left-hand plot is $K^0_L\pi^0$ and the right-hand plot is $K^0_L\omega$. The red histogram is signal, the blue histogram is peaking background, the orange histogram is non-peaking $D^0\overline{D}^0$ background and the green histogram is the continuum background.

4 Double tag results summary

This is a summary of the background-subtracted yield of each double tag. Only statistical uncertainties are shown.

CP+ tags:

- K^+K^-: 19.4 ± 6.3
- $\pi^+\pi^-$: 3.3 ± 8.2
- $K^0_S\pi^0\pi^0$: 18.6 ± 5.1
- $K^0_L\pi^0$: 49.2 ± 10.9
- $K^0_L\omega$: 22.0 ± 6.5

CP− tags:

- $K^0_S\pi^0$: 112.8 ± 11.0
- $K^0_S\eta(\gamma\gamma)$: 18.8 ± 4.5
- $K^0_S\omega$: 41.0 ± 6.7
- $K^0_S\eta(\pi^+\pi^-\pi^0)$: 3.1 ± 2.7
- $K^0_S\eta'(\pi^+\pi^-\eta)$: 9.3 ± 3.2

Mixed-*CP* tags:

- $\pi^+\pi^-\pi^0$: 81.4 ± 15.2
- $4\pi^\pm$ (K^0_S FS < 0): 68.6 ± 18.6
- $4\pi^\pm$ (K^0_S FS < -2): 41.0 ± 16.3
- $4\pi^\pm$ (K^0_S mass veto): 63.0 ± 19.3

Flavour tags:

- $K^\pm\pi^\mp$: 549.6 ± 24.8
- $K^\pm\pi^\mp\pi^0$: 1098.3 ± 35.0

4.1 Systematic uncertainties

4.1.1 Peaking background for $4\pi^{\pm}$ vs $\pi^+\pi^-\pi^0$

The double tag $4\pi^{\pm}$ vs $\pi^+\pi^-\pi^0$ has an important peaking background contribution from $4\pi^{\pm}$ vs $K^0_S\pi^0$. At present the level of this background is estimated by scaling the generic MC sample. However that estimation is biased low. The fact that $4\pi^{\pm}$ is $\sim 75\%$ $CP+$ (from preliminary fits) indicates that the peaking background will be enhanced due to the fact that $K^0_S\pi^0$ is $CP-$.

In general the number of double-tagged $4\pi^{\pm}$ vs $K^0_S\pi^0$ decays is

$$N(4\pi^{\pm}\&K^0_S\pi^0) = \alpha\left[\left(1-F_+^{4\pi^{\pm}}\right)F_+^{K^0_S\pi^0} + \left(1-F_+^{K^0_S\pi^0}\right)F_+^{4\pi^{\pm}}\right] \tag{2}$$

where α encapsulates the branching fractions, efficiencies and overall normalisation.

Events are generated such that the effective F_+ for both tags is 1/2. The number of generated events is thus:

$$N(4\pi^{\pm}\&K^0_S\pi^0)_{\rm Gen} = \alpha\frac{2}{4}. \tag{3}$$

In reality $F_+^{K^0_S\pi^0} = 0$. Setting $F_+^{4\pi^{\pm}} = 0.75$, the actual number of events is

$$N(4\pi^{\pm}\&K^0_S\pi^0)_{\rm Actual} = \alpha\frac{3}{4}. \tag{4}$$

This is a factor of 1.5 larger than the generated quantity.

To account for this difference the fit for this double tag is rerun, increasing the amount of $4\pi^{\pm}$ vs $K^0_S\pi^0$ peaking background by a factor of 1.5. The resulting central value in the number of signal events is 75.5 ± 15.3, compared to the default of 81.4 ± 15.2. This is a shift of approximately 6.

4.1.2 Multiple candidate selection

An alternative multiple candidate selection is used to check for biases. Most double tags are selected based on the average $m_{\rm BC}$, but continuum-dominated ones are selected based on average ΔE. Potential biases are assessed by selecting the candidates randomly, using the same seed to ensure reproducibility.

The influence on the final numbers is minor because most events only have one candidate. The modified numbers are listed below.

$CP+$ tags:

- K^+K^-: 19.4 ± 6.3
- $\pi^+\pi^-$: 3.3 ± 8.2
- $K^0_S\pi^0\pi^0$: 17.5 ± 5.0
- $K^0_L\pi^0$: 49.2 ± 10.9
- $K^0_L\omega$: 22.0 ± 6.5

$CP-$ tags:

- $K^0_S\pi^0$: 112.9 ± 10.8
- $K^0_S\eta(\gamma\gamma)$: 18.8 ± 4.4
- $K^0_S\omega$: 41.1 ± 6.7
- $K^0_S\eta(\pi^+\pi^-\pi^0)$: 3.3 ± 2.7
- $K^0_S\eta'(\pi^+\pi^-\eta)$: 9.3 ± 3.2

Mixed-CP tags:

- $\pi^+\pi^-\pi^0$: 77.9 ± 15.2

- $4\pi^{\pm}$ (K^0_S FS < 0): 64.9 ± 20.2
- $4\pi^{\pm}$ (K^0_S FS < -2): 43.8 ± 16.5
- $4\pi^{\pm}$ (K^0_S mass veto): 63.2 ± 20.2

Flavour tags:

- $K^{\pm}\pi^{\mp}$: 549.7 ± 24.4
- $K^{\pm}\pi^{\mp}\pi^0$: 1060.0 ± 35.0

4.1.3 Dalitz plot acceptance

If the acceptance across the $4\pi^{\pm}$ Dalitz plot is not uniform it might distort the value of F_+ obtained. A model is not available to test the impact of the acceptance so an alternative strategy is pursued.

Using signal MC samples the selection efficiency of each pion in $4\pi^{\pm}$ is determined in bins of $(\mathbf{p}, \theta)$. The events in data are then weighted by the normalised efficiency according to where each pion lies in the phase space. Each pion is treated independently so there are four weights per event. The binning scheme used is as follows:

- $\mathbf{p}$: 0.0–0.3, 0.3–0.5, 0.5–0.7, 0.7–1.0 GeV/c,
- θ: 0.30–1.00, 1.00–1.50, 1.50–2.00, 2.00–2.70 radians.

Events outside the binning are rejected.

The relevant MC sample is used for each double tagged mode. Figure 43 shows example distributions of $\mathbf{p}$ against θ for $4\pi^{\pm}$ vs $K^{\pm}\pi^{\mp}$. The bins are labelled 1–4 from left to right and bottom to top.

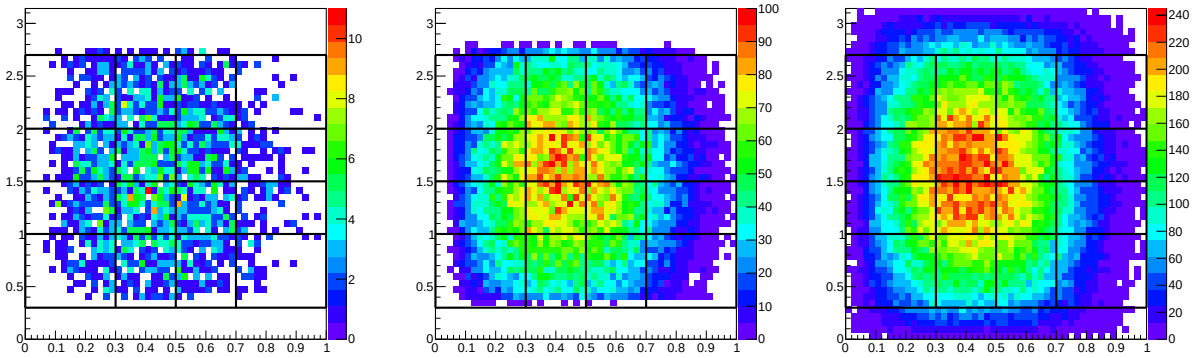

Figure 43: ($\mathbf{p}$, θ) plane for $4\pi^{\pm}$ tagged with $K^{\pm}\pi^{\mp}$: (left) data, (centre) reconstructed MC, (right) generator-level MC. The black grid shows the binning employed.

The pattern of normalised efficiencies is similar for each mode. An example for $4\pi^{\pm}$ vs K^+K^- is shown in Table 15.

The data are weighted and the number of double tags is recomputed. For $4\pi^{\pm}$ vs $4\pi^{\pm}$ both sides of the decay are weighted. The yields are as follows.

CP+ tags:

- K^+K^-: 20.6 ± 6.3
- $\pi^+\pi^-$: 3.5 ± 11.7
- $K^0_S\pi^0\pi^0$: 17.2 ± 4.9
- $K^0_L\pi^0$: 49.9 ± 10.9

	θ bin			
p bin	1	2	3	4
1	0.844 ± 0.004	0.989 ± 0.004	1.003 ± 0.004	0.948 ± 0.005
2	0.967 ± 0.004	1.090 ± 0.003	1.090 ± 0.003	1.052 ± 0.004
3	0.912 ± 0.004	1.078 ± 0.004	1.056 ± 0.004	0.967 ± 0.004
4	0.722 ± 0.007	1.053 ± 0.006	1.005 ± 0.006	0.811 ± 0.007

Table 15: Normalised efficiency for $4\pi^{\pm}$ vs K^+K^-.

- $K^0_L\omega$: 21.5 ± 6.4

CP− tags:

- $K^0_S\pi^0$: 113.8 ± 10.9
- $K^0_S\eta(\gamma\gamma)$: 19.2 ± 4.6
- $K^0_S\omega$: 43.9 ± 6.8
- $K^0_S\eta(\pi^+\pi^-\pi^0)$: 3.7 ± 2.8
- $K^0_S\eta'(\pi^+\pi^-\eta)$: 10.6 ± 3.3

Mixed-*CP* tags:

- $\pi^+\pi^-\pi^0$: 79.9 ± 15.4
- $4\pi^{\pm}$ (K^0_S FS < -2): 38.7 ± 235

Flavour tags:

- $K^{\pm}\pi^{\mp}$: 560.8 ± 25.0

In general the shifts are small. There is a large uncertainty for the $4\pi^{\pm}$ case but the fit appears to have converged properly.

5 Single tag selection results

This section describes the selection of various single tags. Single tags are selected in both data and signal MC. Truth-matched MC is used to determine a signal shape for the resulting fit to data.

5.1 Data yields

The number of single-tag candidates selected in data for each fully-reconstructed decay mode at different selection stages is shown in Table 16. All three $4\pi^{\pm}$ K^0_S vetos are considered.

Decay mode	`DTag`	Cuts	MCS
K^+K^-	71481	15879	15841
$\pi^+\pi^-$	67993	20754	20686
$K^{\pm}\pi^{\mp}$	194392	149822	148331
$K^0_S\pi^0$	71134	27202	26436
$K^0_S\eta$	45776	7570	7110
$K^0_S\omega$	3950437	14039	12845
$K^0_S\eta(\pi^+\pi^-\pi^0)$	3950437	4812	3855
$K^0_S\eta'(\pi^+\pi^-\eta)$	7454	1638	1580
$K^0_S\pi^0\pi^0$	693877	46301	30759
$\pi^+\pi^-\pi^0$	719917	328164	276288
$K^0_S\pi^+\pi^-$	755369	89706	84937
$4\pi^{\pm}$ (K^0_S FS < 0)	1080687	236033	210168
$4\pi^{\pm}$ (K^0_S FS < -2)	1080687	205029	184329
$4\pi^{\pm}$ (K^0_S mass veto)	1080687	253637	224497

Table 16: Candidate yields in data at various stages: '`DTag`' is number from `DTag` software, 'Cuts' is number after selection cuts (including the K^0_S veto where relevant), MCS is number after multiple candidate selection has been applied.

5.2 Single tag MC generation

Signal MC has been generated for various single tags without placing any requirements on what the opposite-side D^0 decays to (i.e. it decays according to `DECAY.DEC`). In the event of non-factorisation of efficiencies, this enables a less biased determination of the single tag efficiency.

5.3 Signal MC fits

Figures 44–49 show a fit to the $m_{\rm BC}$ distribution of each single tag in signal MC. The K^0_S FS cut for $4\pi^{\pm}$ is set to < 0 for the fit shown. The fit function is the sum of a bifurcated Gaussian and another Gaussian. The two PDFs share a common mean. An ARGUS function is used to parameterise the very small amount of non-peaking candidates in each case. The fit is improved by the addition of this shape.

Table 17 shows the yields obtained from the fits, scaled to the signal region in $m_{\rm BC}$. Efficiencies are determined with respect to the number found at generator level. The lepton and shower vetos described in Section 1.5 are applied to the h^+h^- modes.

Table 18 shows the single-tag selection efficiencies for K^+K^-, $\pi^+\pi^-$ and $K^{\pm}\pi^{\mp}$ after removing the lepton and shower vetos.

Table 19 shows a comparison of the product of various single tag efficiencies with the relevant double-tag efficiency. Note that the $4\pi^{\pm}$ K^0_S veto FS cut is set at 0 in all cases. The lepton and shower vetoes are not applied to the h^+h^- modes.

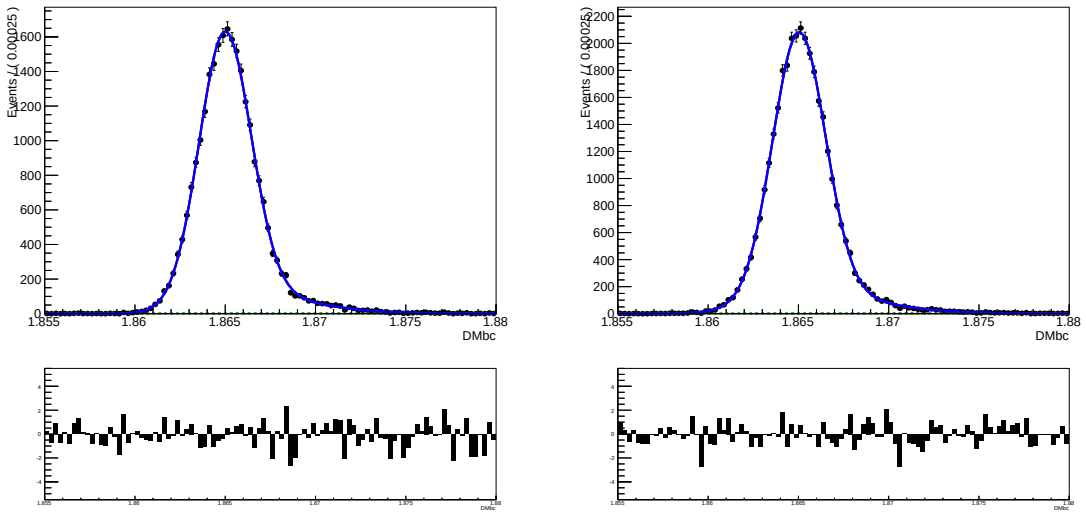

Figure 44: Fit to single tag $m_{\rm BC}$ distribution in signal MC for (left) K^+K^- (right) $\pi^+\pi^-$.

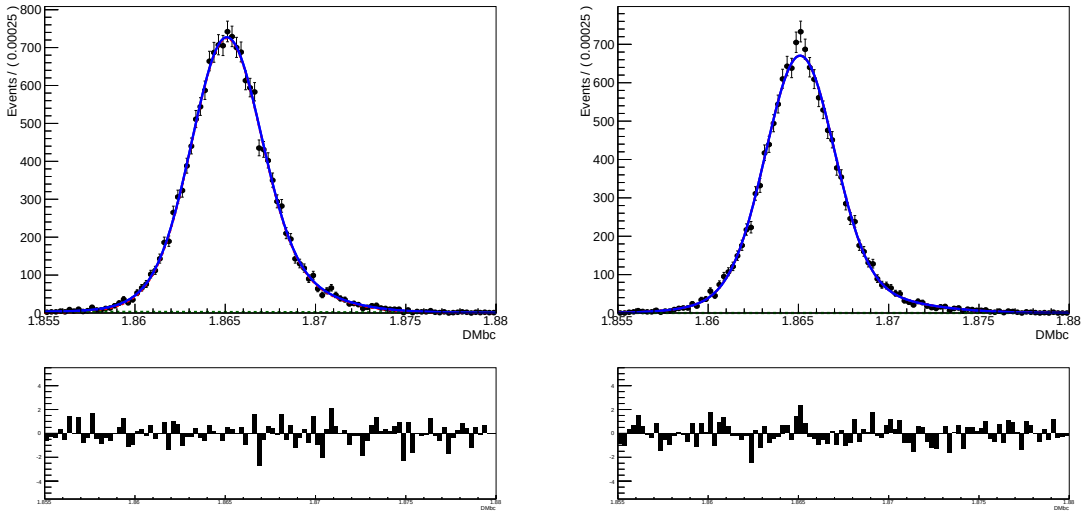

Figure 45: Fit to single tag $m_{\rm BC}$ distribution in signal MC for $K^0_S\pi^0$ (right) $K^0_S\eta(\gamma\gamma)$.

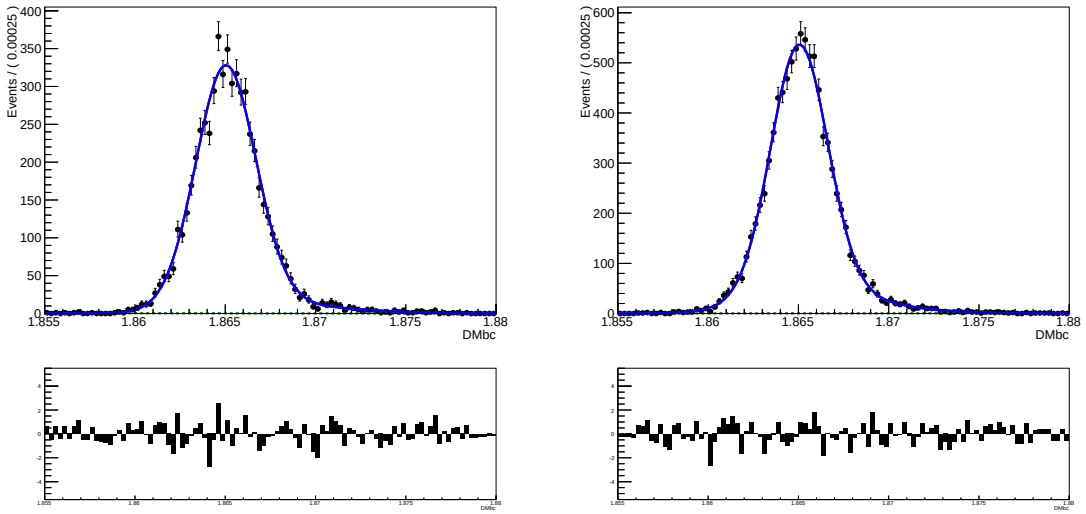

Figure 46: Fit to single tag $m_{\rm BC}$ distribution in signal MC for (left) $K^0_S\omega$ (right) $K^0_S\eta(\pi^+\pi^-\pi^0)$.

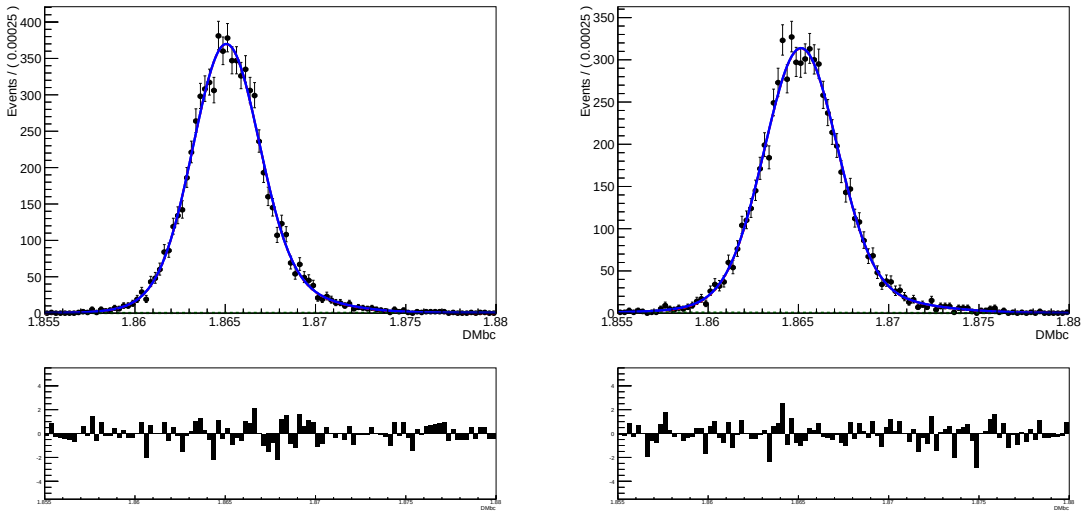

Figure 47: Fit to single tag $m_{\rm BC}$ distribution in signal MC for (left) $K^0_S\eta'(\pi^+\pi^-\eta)$ (right) $K^0_S\pi^0\pi^0$.

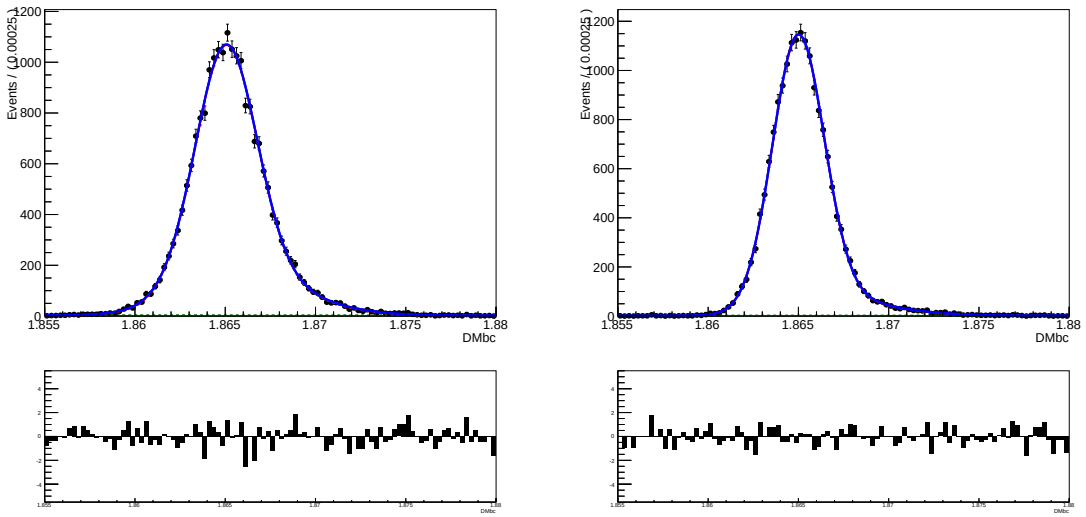

Figure 48: Fit to single tag $m_{\rm BC}$ distribution in signal MC for (left) $\pi^+\pi^-\pi^0$ (right) $K^0_S\pi^+\pi^-$.

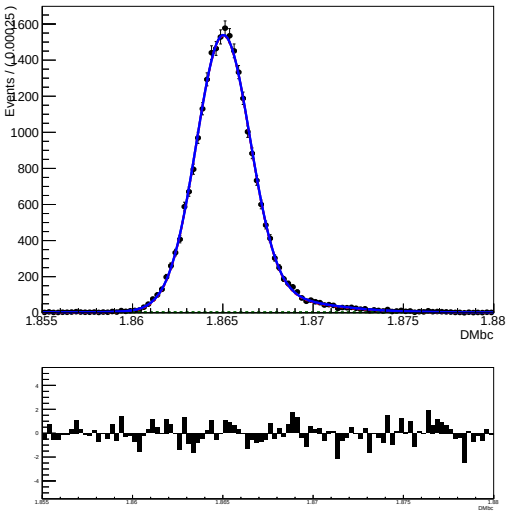

Figure 49: Fit to single tag $m_{\rm BC}$ distribution in signal MC for $4\pi^{\pm}$.

Decay mode	Efficiency (%)
K^+K^-	49.5 ± 0.3
$\pi^+\pi^-$	64.7 ± 0.4
$K^\pm\pi^\mp$	58.2 ± 0.3
$K^0_S\pi^0$	29.6 ± 0.2
$K^0_S\eta(\gamma\gamma)$	26.8 ± 0.2
$K^0_S\omega$	13.0 ± 0.2
$K^0_S\eta(\pi^+\pi^-\pi^0)$	18.0 ± 0.2
$K^0_S\eta'(\pi^+\pi^-\eta)$	14.2 ± 0.2
$K^0_S\pi^0\pi^0$	13.8 ± 0.2
$\pi^+\pi^-\pi^0$	41.5 ± 0.3
$4\pi^\pm$ (K^0_S FS < 0)	49.9 ± 0.3
$4\pi^\pm$ (K^0_S FS < -2)	43.3 ± 0.4
$4\pi^\pm$ (K^0_S mass veto)	53.7 ± 0.4
$K^0_S\pi^+\pi^-$	34.7 ± 0.3

Table 17: Single tag efficiency obtained from fits to signal MC.

Decay mode	Efficiency (%)
K^+K^-	56.8 ± 0.3
$\pi^+\pi^-$	70.9 ± 0.4
$K^\pm\pi^\mp$	63.7 ± 0.4

Table 18: Single tag efficiency obtained from fits to signal MC for h^+h^- modes, removing the lepton and shower vetos.

Decay mode	ST eff. (%)	ST eff. $\times$ $4\pi^\pm$ ST eff. (%)	DT eff. (%)	Ratio (ST$\times$ST/DT)
K^+K^-	56.8 ± 0.3	28.3 ± 0.2	27.2 ± 0.2	1.04 ± 0.01
$\pi^+\pi^-$	70.9 ± 0.4	35.4 ± 0.3	34.0 ± 0.2	1.04 ± 0.01
$K^\pm\pi^\mp$	63.7 ± 0.4	31.8 ± 0.3	31.0 ± 0.2	1.03 ± 0.01
$K^0_S\pi^0$	29.6 ± 0.2	14.8 ± 0.1	14.0 ± 0.2	1.06 ± 0.02
$K^0_S\eta(\gamma\gamma)$	26.8 ± 0.2	13.4 ± 0.1	12.9 ± 0.2	1.04 ± 0.02
$K^0_S\omega$	13.0 ± 0.2	6.5 ± 0.1	6.1 ± 0.1	1.06 ± 0.02
$K^0_S\eta(\pi^+\pi^-\pi^0)$	18.0 ± 0.2	9.0 ± 0.1	8.5 ± 0.1	1.06 ± 0.02
$K^0_S\eta'(\pi^+\pi^-\eta)$	14.2 ± 0.2	7.1 ± 0.1	6.8 ± 0.1	1.04 ± 0.02
$K^0_S\pi^0\pi^0$	13.8 ± 0.2	6.9 ± 0.1	6.5 ± 0.1	1.06 ± 0.02
$\pi^+\pi^-\pi^0$	41.5 ± 0.3	20.7 ± 0.2	20.1 ± 0.2	1.03 ± 0.01
$4\pi^\pm$	49.9 ± 0.3	24.9 ± 0.2	20.3 ± 0.2	1.23 ± 0.02
$K^0_S\pi^+\pi^-$	34.7 ± 0.3	17.3 ± 0.2	15.7 ± 0.2	1.10 ± 0.02

Table 19: Test for factorisation of selection efficiency. For $4\pi^\pm$ the K^0_S veto requires FS < 0.

In each case the product of the two single tag efficiencies is larger than the respective double tag efficiency. For *CP* tags the discrepancy is 3–6%. The discrepancy for $K^0_S\pi^+\pi^-$ is larger but is not important because the normalisation is floated in that mode.

The discrepancy for $4\pi^\pm$ tagged with itself is very large. The reason for this stems from the method used to select multiple candidates. The discriminating variable is the average ΔE. This pushes some of the signal into the diagonal (C) sideband on the $m_{\rm BC}$ plane. If instead the average $m_{\rm BC}$ is used to select multiple candidates, the double tag efficiency becomes 22.5 ± 0.2. The ratio of the squared $4\pi^\pm$ single tag efficiency to the double tag efficiency then becomes 1.11 ± 0.01 which is more in line with the other modes; it is most similar to $4\pi^\pm$ vs $K^0_S\pi^+\pi^-$. The use of $m_{\rm BC}$ for multiple candidate selection is not possible for this mode because that variable is used in the fit to discriminate between the signal and large continuum background.

The $4\pi^\pm$ vs $4\pi^\pm$ result shown is for the K^0_S veto with a FS cut < 0. If the veto is set to < -2, the ratio becomes 1.23 ± 0.02. If a mass veto is applied instead, the ratio becomes 1.22 ± 0.02. The degree of non-factorisation is therefore consistent for different K^0_S cuts.

If the multiple candidate selection is not applied, a similar ratio is found: 1.18 ± 0.02 (for a K^0_S FS cut < 0). This still exhibits a large degree of non-factorisation; it is not quite the same as with the multiple candidate selection due to the effects discussed above. Therefore the non-factorisation seems to be robust against the various selections that are applied.

The procedure is tested by generating some $K^\pm\pi^\mp$ vs $K^\mp\pi^\pm$ Monte Carlo. The double tag efficiency is 41.2 ± 0.2. The square of the $K^\pm\pi^\mp$ single tag efficiencies (without the shower and lepton vetos) is 40.6 ± 0.4. The ratio between the two is 1.01 ± 0.01 which is only slightly biased high. This indicates that the method is sound, helping to confirm the non-factorisation appearing in the $4\pi^\pm$ double tags.

The effective single tag efficiencies for the K^0_L *CP* tags are obtained by dividing the double tag efficiencies by the single tag $4\pi^\pm$ efficiency. A correction factor of 1.05 ± 0.02 is applied to this ratio based on the values obtained for the fully-reconstructed *CP* tags. These efficiencies can then be converted to single tag yields by multiplying by $2N_{D^0\bar{D}^0}$ and the branching fraction of the mode in question, correcting for MC-data differences (see Section 5.4 for more details). The branching fraction for D^0 decays to $K^0_L\omega$ is assumed to be equal to that of decays to $K^0_S\omega$. The efficiencies and single tag yields are listed in Table 20. (The numbers

Decay mode	ST eff. (%)	ST yield
$K^0_L\pi^0$	41.7 ± 0.9	23420 ± 1813
$K^0_L\omega$	15.8 ± 0.4	8782 ± 536

Table 20: Effective single tag efficiencies and yields for the K^0_L modes.

are very compatible with those in the $h^+h^-\pi^0$ paper, bearing mind most inputs are uncorrelated with this study.)

5.4 Data fits

Figures 50–55 show a fit to the $m_{\rm BC}$ distribution of each single tag in data. The signal PDF is the one used in Section 5.3, but the mean and width of the single Gaussian are allowed to float. If this is not done the fit pulls are bad for many of the modes, mainly due to an offset in the mean. The floating Gaussian width allows more flexibility to describe the high-$m_{\rm BC}$ tail which is caused by ISR and may not be correctly modelled in MC. The background shape is an ARGUS PDF with all shapes floating except the threshold. The $4\pi^\pm$ FS cut is set to < 0.

5.5 Results

The single tag yields are shown in Table 21. The numbers are scaled to the signal region ($1.86 \leq m_{\rm BC} \leq 1.87$ GeV/c^2) in order to match the range used in the double tag selections. The single tag yields are compared to those calculated with the simple formula $S(X) = 2N_{D^0\bar{D}^0}\mathcal{B}(X)\varepsilon(X)c(X)$. The parameter $c(X)$ is the MC-data correction factor equal to 0.940 ± 0.013 for each π^0 candidate in the final state and 0.944 ± 0.040 for each $\eta(\gamma\gamma)$.

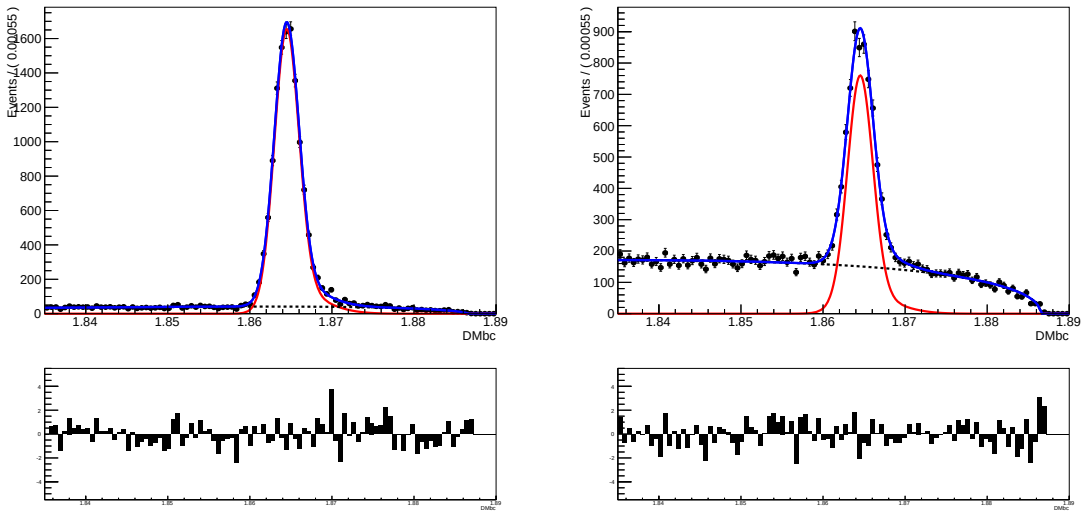

Figure 50: Fit to single tag $m_{\rm BC}$ distribution in data for (left) K^+K^- (right) $\pi^+\pi^-$.

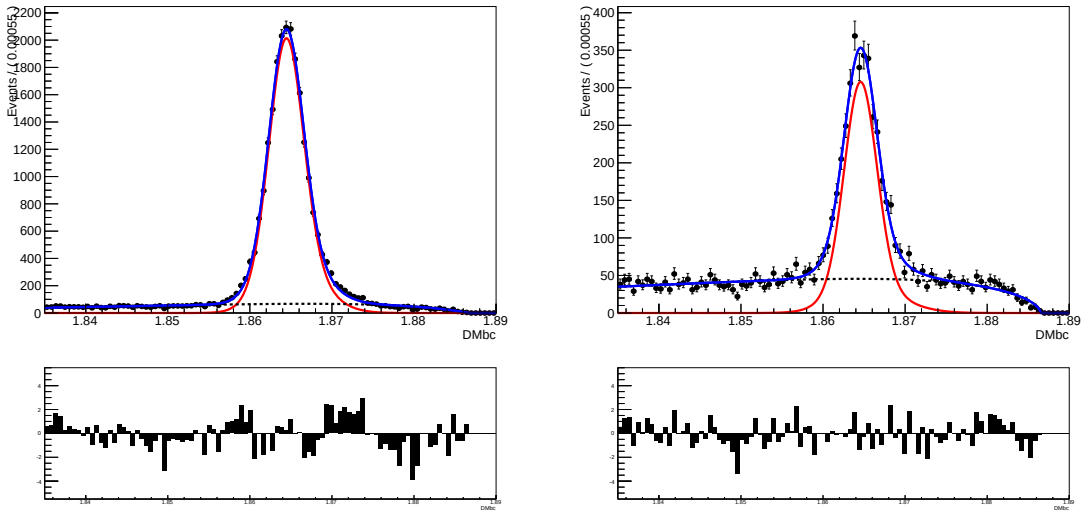

Figure 51: Fit to single tag $m_{\rm BC}$ distribution in data for $K^0_S\pi^0$ (right) $K^0_S\eta(\gamma\gamma)$.

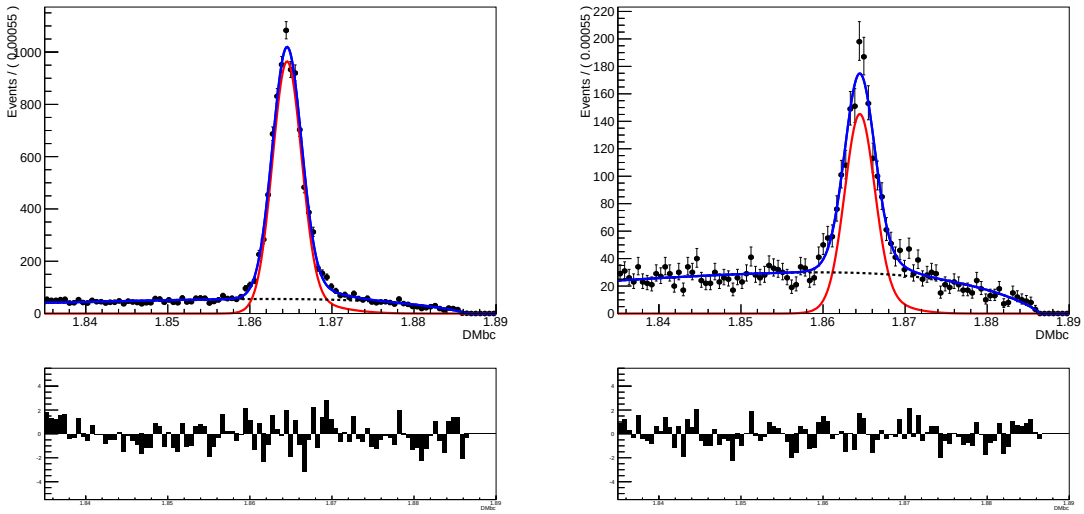

Figure 52: Fit to single tag $m_{\rm BC}$ distribution in data for (left) $K^0_S\omega$ (right) $K^0_S\eta(\pi^+\pi^-\pi^0)$.

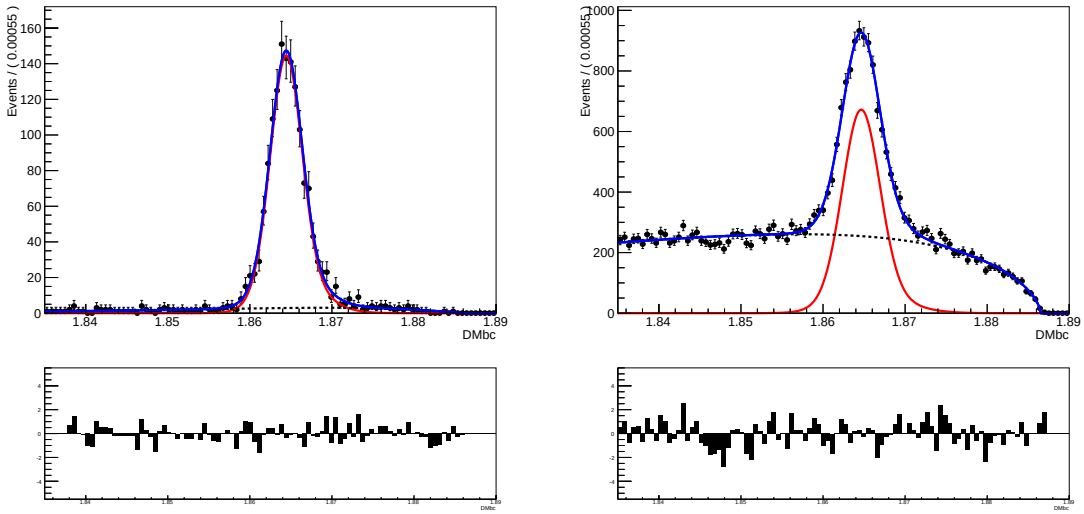

Figure 53: Fit to single tag $m_{\rm BC}$ distribution in data for (left) $K^0_S\eta'(\pi^+\pi^-\eta)$ (right) $K^0_S\pi^0\pi^0$.

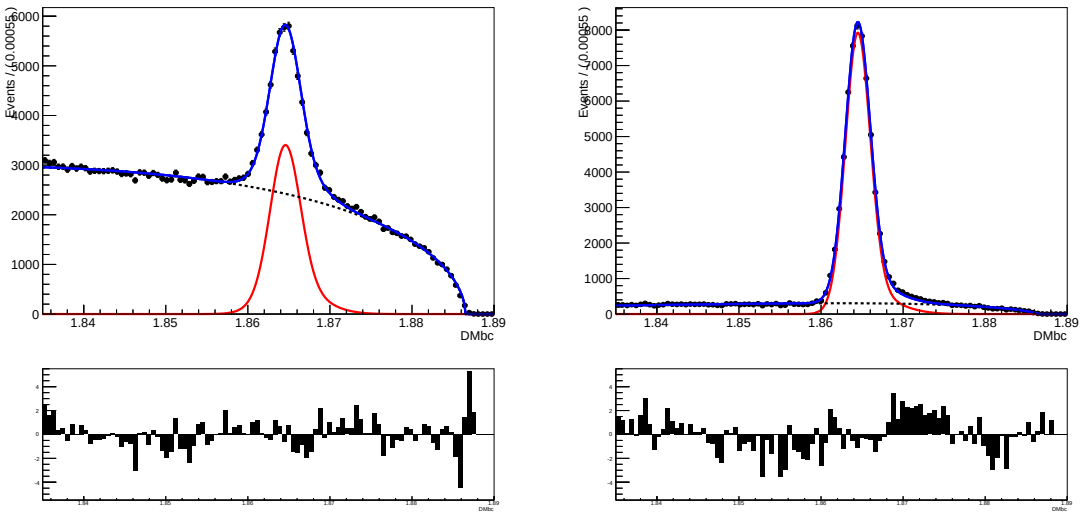

Figure 54: Fit to single tag $m_{\rm BC}$ distribution in data for (left) $\pi^+\pi^-\pi^0$ (right) $K^0_S\pi^+\pi^-$.

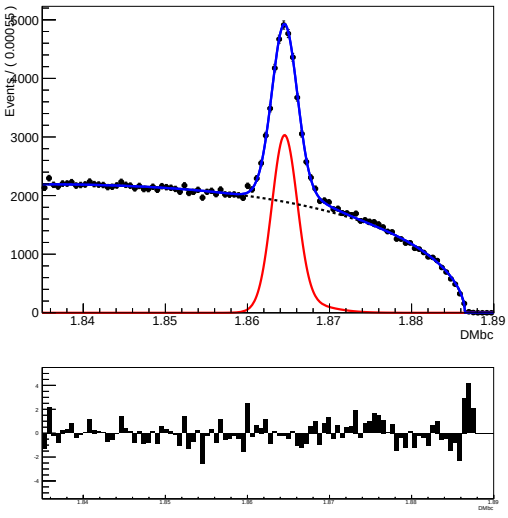

Figure 55: Fit to single tag $m_{\rm BC}$ distribution in data for $4\pi^{\pm}$.

Decay mode	Single tag yield	$2N_{D^0\bar{D}^0}\mathcal{B}(X)\varepsilon(X)c(X)$
K^+K^-	11891 ± 115	11722 ± 355
$\pi^+\pi^-$	5618 ± 97	5424 ± 141
$K^\pm\pi^\mp$	131736 ± 369	135038 ± 3417
$K^0_S\pi^0$	19981 ± 147	19800 ± 854
$K^0_S\eta(\gamma\gamma)$	2908 ± 68	2856 ± 226
$K^0_S\omega$	7976 ± 97	7234 ± 428
$K^0_S\eta(\pi^+\pi^-\pi^0)$	1248 ± 46	1032 ± 96
$K^0_S\eta'(\pi^+\pi^-\eta)$	1322 ± 39	1274 ± 93
$K^0_S\pi^0\pi^0$	6993 ± 135	6636 ± 833
$\pi^+\pi^-\pi^0$	30459 ± 324	33359 ± 1643
$K^0_S\pi^+\pi^-$	57307 ± 260	58724 ± 4383
$4\pi^\pm$ (K^0_S FS < 0)	22201 ± 261	22141 ± 791
$4\pi^\pm$ (K^0_S FS < -2)	18836 ± 243	19213 ± 699
$4\pi^\pm$ (K^0_S mass veto)	22800 ± 269	23828 ± 858

Table 21: Yield of single tags in the signal region.

Good agreement is observed. There are other effects such as fit systematics and mixing that if included would change the central values and/or uncertainties a little.

5.6 Self-tagged $4\pi^\pm$

The expected relationship between the number of single-tagged $4\pi^\pm$ candidates, the number of self-tagged $4\pi^\pm$ candidates, and the fraction $F_+^{4\pi^\pm}$ is

$$F_+^{4\pi^\pm}\left(1 - F_+^{4\pi^\pm}\right) \sim \frac{1.23 N_{D^0\bar{D}^0} N(4\pi^\pm \& 4\pi^\pm)}{S(4\pi^\pm)^2} \tag{5}$$

where the non-factorisation of the efficiencies is taken into account with the factor 1.23.

The values of $F_+^{4\pi^\pm}\left(1 - F_+^{4\pi^\pm}\right)$ obtained for each K^0_S veto are

- K^0_S FS < 0: 0.51 ± 0.14
- K^0_S FS < -2: 0.42 ± 0.17
- K^0_S mass veto: 0.45 ± 0.14

The theoretical maximum is 0.25; these values are 1–2 σ above that, and a little more above the value 0.1875 which is obtained when $F_+ = 0.75$.